Recent advances on catalytic osmium-free olefin syn-dihydroxylation

Thierry Achard, Stéphane Bellemin-Laponnaz

Recent advances on catalytic osmium-free olefin *syn*-dihydroxylation.

Thierry Achard,* [a] and Stéphane Bellemin-Laponnaz* [a]

[a] Dr. T. Achard, Dr. S.Bellemin-Laponnaz
Département des Matériaux Organiques
Institut de Physique et Chimie des Matériaux de Strasbourg (IPCMS) Université de Strasbourg, CNRS UMR-7504
23 rue du Loess, BP 43, 67034 Strasbourg Cedex 2, France
E-mail: thierry.achard@ipcms.unistra.fr; bellemin@unistra.fr

Abstract: The *syn*-dihydroxylation of olefinic group is one of the most important synthetic transformations which leads to the controlled formation of syn-diol. Such 1,2-diol structure is integrated into more complex architectures and substantially participates in the development of biologically active molecules and other fine chemicals. This minireview describes recent evolution of this research field in the past decade, surveying osmium-free and more eco-compatible system and in particular the direct oxidation of olefins catalyzed by transition metal complexes.

1. Introduction

The *syn*-diol pattern and 1,2 in particular is one of the most ubiquitous motif in natural compounds. They are found in several biomolecules such as sugars, carbohydrates, nucleosides and catecholamines, which mediate a diverse array of biological processes.[1] The *syn*-relationship between the two hydroxyl groups allows them to participate in various biochemical reactions and necessary life activities.[2] This *syn*-diol pattern is also found in many biological active molecules such as aminoglycoside antibiotics, flavonoid glycosides, polyketides and alkaloids derivatives (Figure 1).[3] Finally, *syn*-diols serve as valuable building blocks for pharmaceuticals, agrochemicals and in the design of chiral ligand for transition-metals catalysts.[3-4]

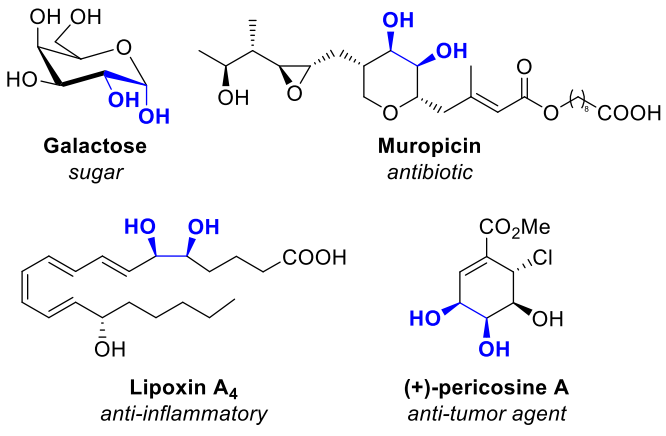

Figure 1. Examples of natural products and synthetic biologically active compounds containing a *syn*-1,2-diol unit.

For all these reasons, the vicinal dioxygenation of alkenes is one of the most significant organic transformations because it generates the desired *syn*-diol in one direct step. However to achieve *syn*-diols, the dioxygenation of the alkene precursor should be in a stereoselective manner and various strategies have been developed since the beginning of the 19th century.

The discovery by Hoffmann in 1912 of the oxidation of unsaturated species by osmium tetroxide paved the way of the dihydroxylation of alkenes.[5] Latter Criegee developed an effective *cis*-dihydroxylation where OsO_4 was used stoichiometrically with no other oxidant.[6] Several improvements have been made and the two most remarkable advances have been described by Upjohn who made it possible to achieve catalytic reactions with osmium and, later on, by Sharpless for the asymmetrical version of the reaction.[7] The great generality and selectivity of this reaction makes it the most used methodology.

On the other hand, the toxicity, volatility and cost of such osmium reagent have prompted organic chemists to develop new processes using more eco-compatible and environmentally friendly catalysts and oxidants.[8] These *syn*-dihydroxylation reactions are mainly based on two strategies involving either transition-metal catalysts[8] or metal-free[9] procedures. As example, *syn*-diols have been obtained from alkenes, under transition-metal-free conditions,[9] using different oxidants such as iodine derivatives,[10] oxone®[11] or cyclic diacyl peroxides.[12] In addition, selenium compounds such as SeO_2 or *in situ* generated $PhSeOSO_3H$ are also able to *syn*-dioxygenate olefins.[13] Sulfur-reagents have also been reported but these remain significantly less developed.[14]

Since the last comprehensive review on osmium-free *syn*-dihydroxylation by Bataille and Donohoe in 2011,[8] many notable advances have been made to directly generate 1,2-*syn*-diol units from alkene precursors with no need of osmium-based reagents. The aim of this mini-review is to give an up-to-date on the most recent efforts done to explore the metal-catalyzed *syn*-dihydroxylation of olefins, and highlight their advantages and/or disadvantages in order to present the best catalytic systems described so far.

Thierry Achard studied chemistry at the University of Aix-Marseille. In 2002, he joined the group of Professor Michael North and obtained his PhD in 2006 at King'sCollege London/Newcastle University while studying the development of new chiral metal(salen) complexes. In 2006 he joined the group of Prof. Antoni Riera at the Institute for Research in Biomedecine (Barcelona) as a postdoctoral fellow in asymmetric metal-catalysis cycloaddittion. In 2008, he became

a postdoctoral fellow in the group of Prof. Gérard Buono at the Aix-Marseille university to develop tandem cyclization reactions. In early 2011, he was post-doctoral fellow with Prof. Jérôme Lacour in Genève University, where he developed catalytic carbenoid insertion reactions. Finally in 2014, he was appointed as CNRS researcher in the team of Dr. Stéphane Bellemin-Laponnaz at the University of Strasbourg at the IPCMS. His research focuses in particular on the development of new chiral ligands, organometallic/coordination complexes and on new catalytic systems more respectful of the environment.

Stéphane Bellemin-Laponnaz studied chemistry at Université Joseph Fourier (Grenoble) and Université Louis Pasteur (Strasbourg). In 1994, he joined the group of Professor John A. Osborn at Université Louis Pasteur to obtain his doctorate in 1998 while studying the chemistry of oxo compounds. In 1999, he became a member of the group of Professor Gregory C. Fu at Massachusetts Institute of Technology (Cambridge, MA) as a postdoctoral fellow working on asymmetric catalysis. In late 2000, he joined the group of Professor Lutz H. Gade at Université Louis Pasteur as CNRS researcher and joined the Institut de Physique et Chimie des Matériaux de Strasbourg as CNRS Director of Research in 2010. His research focus on organometallic chemistry, coordination chemistry and homogeneous catalysis. He was awarded a Bronze Medal by the CNRS in 2005, Coordination Chemistry Prize of the Société Chimique de France in 2009 and Sandmeyer Prize of the Swiss Chemical Society in 2013.

2. Ruthenium-mediated *syn*-dihydroxylation

Most often $RuCl_3$ hydrate or ruthenium dioxide are used as pre-catalysts concomitant together with a co-oxidant ($NaIO_4$) to generate the “ruthenium oxide” active species (i.e. ruthenium tetroxide and insoluble low-valent ruthenium-carboxylate complexes formed during the course of the reaction). However, due to its high oxidizing power, it often leads to successive oxidative transformations which decrease the selectivity of the diol. As a result, its use is more widespread within the synthetic community for reaction of ketohydroxylation to generate hydroxy ketones and oxidative cleavage reactions to give the corresponding carbonyl compounds.[15] The mechanism indicates a concerted [3+2]-cycloaddition between the olefin and RuO_4 (**I**) to lead to ruthenium intermediate (**II**) which is oxidized to ruthenate **III** (Figure 2). This cyclic ruthenium-ester plays a key role in all transformations. The nucleophilic addition of water leads to the formation of the expected diol. Therefore, if the hydrolysis of ruthenate is too slow, the ruthenium intermediates **II** and **III** might prefer the fragmentation pathway towards the aldehyde. Even if the ruthenium tetroxide was often considered as a too strong oxidant, the last twenty years have still shown various improvements in dihydroxylation of alkenes by RuO_4.

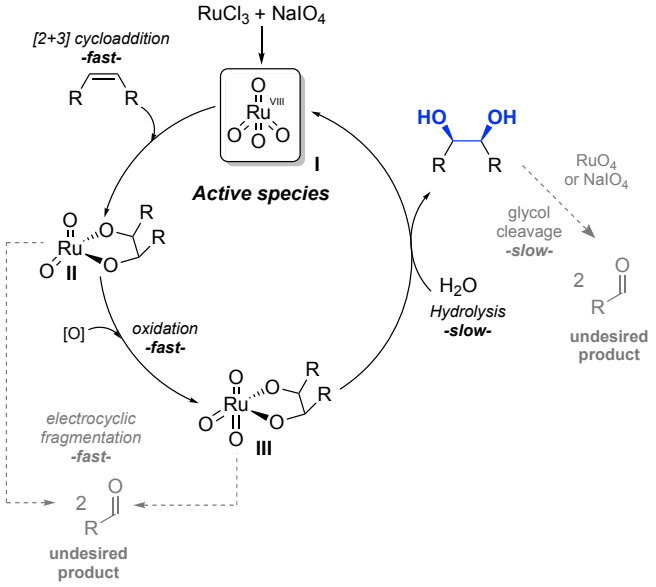

Figure 2. Mechanism for ruthenium-catalyzed *syn*-dihydroxylation and possible competitive pathways.

2.1. Conventional methods using RuO_4

Similar to OsO_4, the ruthenium tetroxide (RuO_4) complex is also able to oxidize alkene substrates. Since the seminal reported by Sharpless and Akashi on the *syn*-addition of RuO_4 to olefins, ruthenium tetroxide is now commonly used in direct *syn*-dihydroxylation (Scheme 1).[16] Using acetone-water as solvent, improved product yields were reported by Sicca on steroid derivatives.[17] However, it was in 1994 that a major breakthrough, called "flash dihydroxylation", was achieved by Shing and co-workers which allowed this oxidative process of being catalytic with very short reaction times (<4 min).[18] Addition of catalytic amounts of a Brønsted acid or $CeCl_3$ to the reaction mixture improved this transformation and allowed a decrease of the catalyst loading up to 0.25 mol% as showed by Plietker *et al* (Scheme 1).[19] In fact, the presence of the acid leads to a faster hydrolysis of ruthenate ester **III** species, thus promoting the formation of the diol. Many examples have been reported in the literature using such systems.[20]

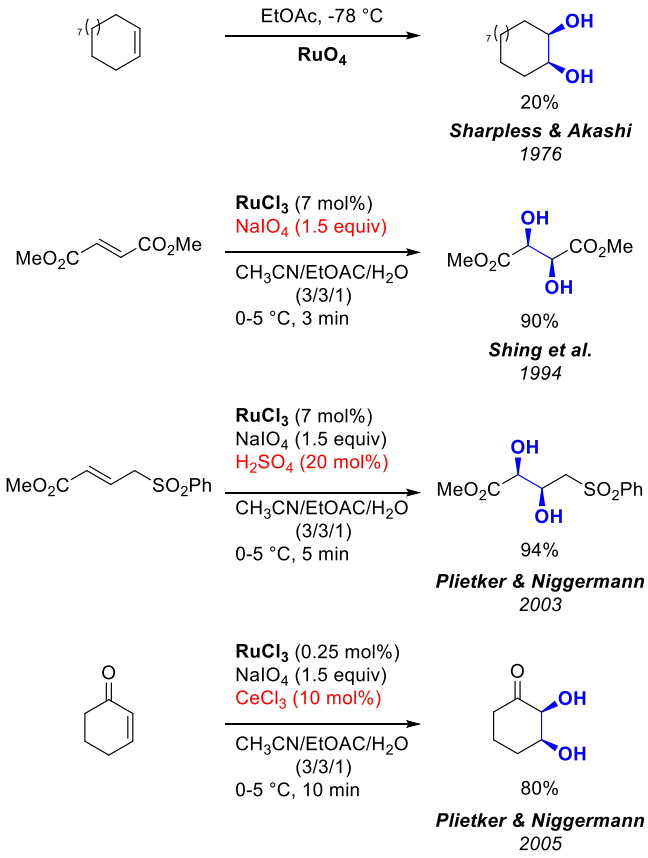

Scheme 1. Stoichiometric and catalytic *syn*-dihydroxylation using RuO_4 or *in situ* generated RuO_4.

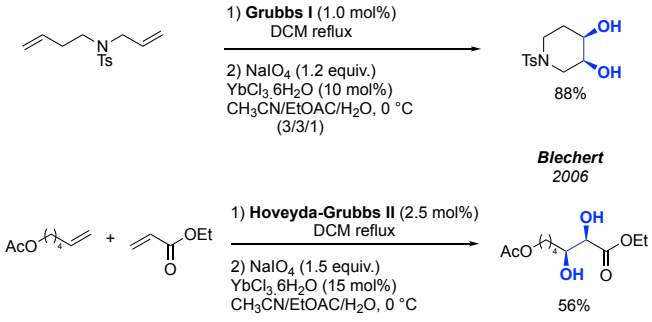

Scheme 2. RCM/dihydroxylation and CM/dihydroxylation procedure.[21]

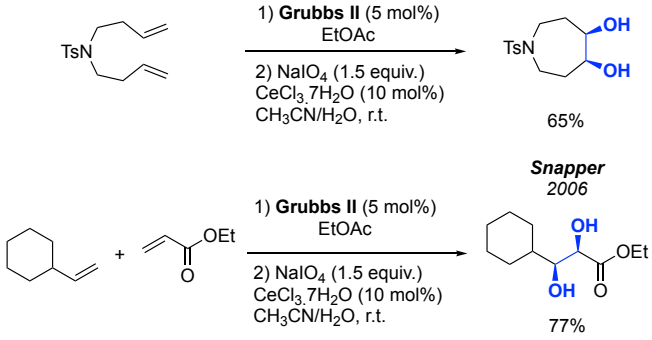

Scheme 3. RCM/dihydroxylation and CM/dihydroxylation procedure.[22]

2.2. Tandem reaction metathesis/dihydroxylation procedures

The literature contains a few reports of assisted tandem catalysis where a single catalyst is able to perform multiple transformations. In all cases, the *syn*-dihydroxylation reaction takes place after the first (catalyzed) transformation by reaction with the alkene product. This second transformation is always triggered by the addition of an appropriate oxidant.

2.2.1 Metathesis/dihydroxylation

This field has been first explored by Blechert *et al.* in 2006 for Ru-mediated sequential Ring Closing Metathesis (RCM)/dihydroxylation and Cross Metathesis (CM)/dihydroxylation sequence (Scheme 2).[21] The authors generated the active RuO_4 from the well-established pre-catalyst Grubbs I (RCM) or Hoveyda-Grubbs I (CM) in presence of $NaIO_4$ and 10-15 mol% of $YbCl_3$. Since then, this strategy has been successfully used and improved by Snapper by eliminating the solvent and subsequent addition of $CeCl_3$ (Scheme 3).[22] Neisius and Plietker reported a diastereoselective dihydroxylation of olefins *via* a tandem cross metathesis/dihydroxylation sequence, in presence of a chiral auxiliary attach to one alkene.[23]

This elegant RCM/dihydroxylation strategy has been successfully applied to the synthesis of more sophisticated polyhydroxylated quinolizidines backbone by Jarosz *et al* (Scheme 4).[24] The authors applied the conditions described by Plietker, using $NaIO_4/CeCl_3$, to the Grubbs II catalyst in order to reduce the high reactivity of RuO_4 formed.[19] The diol resulting from the bis-allyl piperidine compound was obtained in 69% yield as a mixture of the diastereomers **1a** and **1b** in a 1:4.3 ratio. Trifluoroacetic acid (TFA) was used during the RCM step to form the ammonium/TFA salt *in situ* in order to circumvent the known deactivation of the Grubbs II catalyst by free amine (scheme 4a). Interestingly, a reverse ratio (**1a/1b**, 3.5:1) was observed when the dihydroxylation step was done with OsO_4 (5 mol%). An acryloyl analogue **2a-b** could also be obtained, without TFA, in good yield (74%) but in this case poor diastereoselectivity was noticed (**2a**/**2b**, 1:1.4) (scheme 4b).

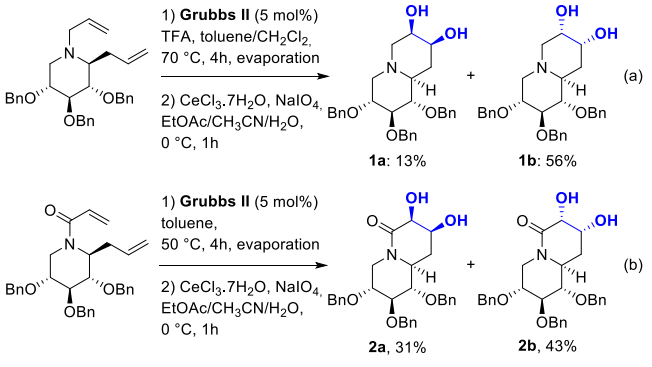

Scheme 4. Synthesis of polyhydroxylated quinolizidines *via* tandem RCM/*syn*-dihydroxylation. [24]

Starting from D-xylose bis-allyl substrates (Scheme 5) were prepared in several steps. Efficient tandem RCM/dihydroxylation was observed only if the OH group from the allylic alcohol was protected. With this sequence either quinolizidine **3** (Scheme 5a) or azepine **4** (Scheme 5b) bicyclic-type backbone were efficiently generated (Scheme 5).[25] In each case the transformations proceed with very high diastereoselectivities generating the *syn*-diol as a single diastereomer.

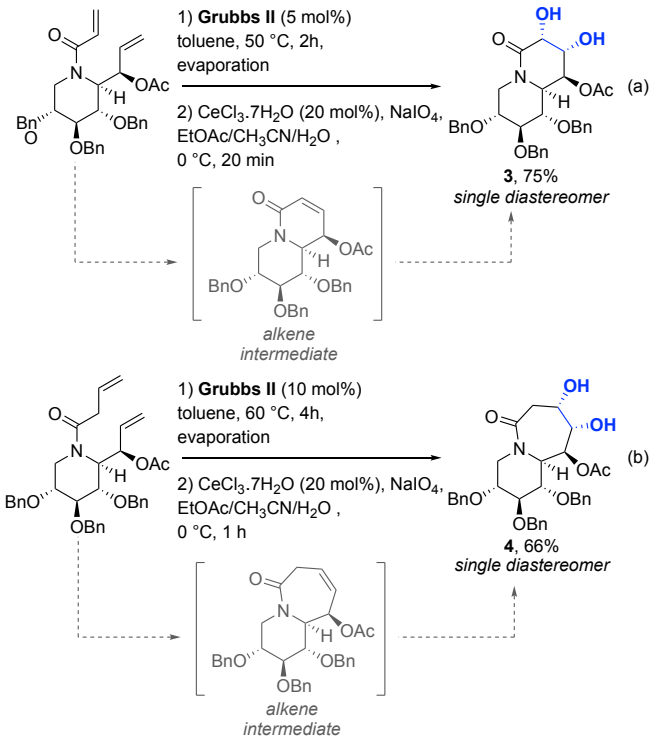

Scheme 5. Synthesis of polyhydroxylated derivatives of quinolizidine and decahydropyrido[1,2-a]azepine by tandem RCM/dihydroxylation procedures. [25]

A year later the same author reported the synthesis of optically pure polyhydroxylated *trans*-decalins **5-6** through a sequence of a one-pot 1,4-addition/aldol reaction and RCM/*syn*-dihydroxylation (Scheme 6a-b).[26] Desired *syn*-diols were obtained, from two different diastereomers, with moderate overall yield but with good to high diastereoselectivity respectively. To explain the observed high selectivity the author suggested that the *syn*-dihydroxylation proceeded from the less congested face of the double bond (*anti* compared to the neighboring benzoyl group, see scheme 6c).

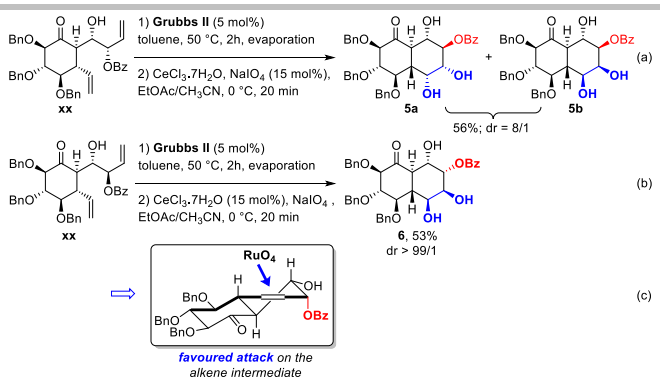

Scheme 6. Synthesis of polyhydroxylated *trans*-decalin *via* tandem RCM/*syn*-dihydroxylation. In the box, the preferential attack of RuO_4 to the less hinderer face of the double bond. [26]

2.2.2 Glycosylation/dihydroxylation

In 2014, Kashyap and co-workers reported a one-pot glycosylation-dihydroxylation sequence to access α-D-mannopyranosides from glycals (Scheme 7).[27] The glycosylation stage shows a wide tolerance to various acceptors ranging from conventional alcohol, passing through hydroxylamine and even up to sugar and alcohols derived from amino acids. The reaction proceeded smoothly to give first the corresponding 2,3-unsaturated glycosides intermediate (Scheme 7) which is then attacked by the in-situ generated RuO_4 species to give the *syn*-diols **7a-b**. Finally a final acetylation step provides access to α-D-mannopyranoside **8a** as major product and β-allopyranoside **8b** as minor product (Scheme 7). The stereoselectivity observed is explained by the authors by the anomeric effect and the equilibrium between the kinetic and the thermodynamic oxocarbenium intermediate (see Scheme 8) which is probably responsible to the formation of the axial anomer. Then, the [3+2]-*syn*-cycloaddition of RuO_4 onto the olefin occurs in the less hindered face: anti of the newly entered OR group (in the same way as Scheme 6).

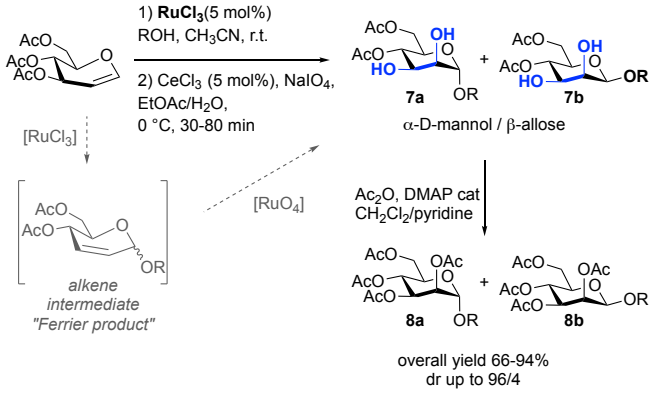

Scheme 7. One-pot glycosylation/*syn*-dihydroxylation catalysed by $RuCl_3$. [27]

The authors have successfully applied the same strategy with thiols which gave α-D-mannopyranosyl sulfones with good yield

and very high regioselectivity. In this sequence, the oxidation of the thioether takes place before the oxidation of the double bond and after the formation of a 2,3-unsaturated α-glycoside through the glycosylation of Ferrier[28] (Scheme 8).[20c]

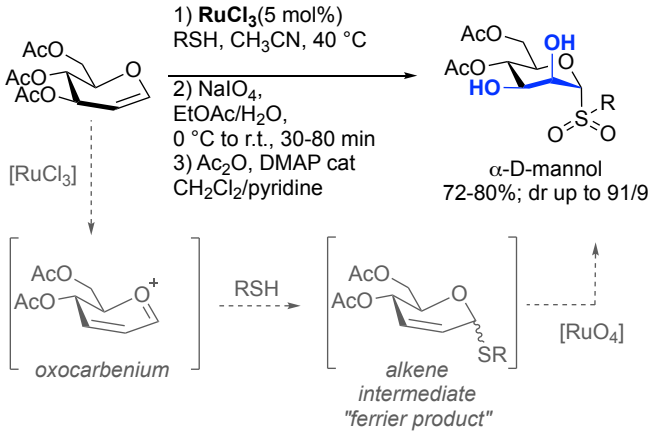

Scheme 8. Synthesis of mannopyranosyl sulfones *via* sequential glycosylation/thio-oxydation/*syn*-dihydroxylation catalyzed by $RuCl_3$. [20c]

A mechanism was proposed, for this $RuCl_3$-catalyzed one-pot glycosylation-dihydroxylation, which would start with the Ru-activation of the C3-acetate in **IV** (Scheme 9). This would drive the formation of allyloxycarbenium ion **V**. Preferentially attack of the alcohol nucleophile from the α-face to this half chair conformation carbenium ion would conduct to the preferential formation of 2,3-unsaturated α-glycosides **VI**, probably due to both anomeric effect and steric effect. Finally, the oxidation of Ru(III) to RuVIII by IO_4 was then followed by [3+2]-*syn*-cycloaddition of RuO_4 on the olefin via the less sterically hindered face, which should provide the desired 1,2-diol **VIII**.

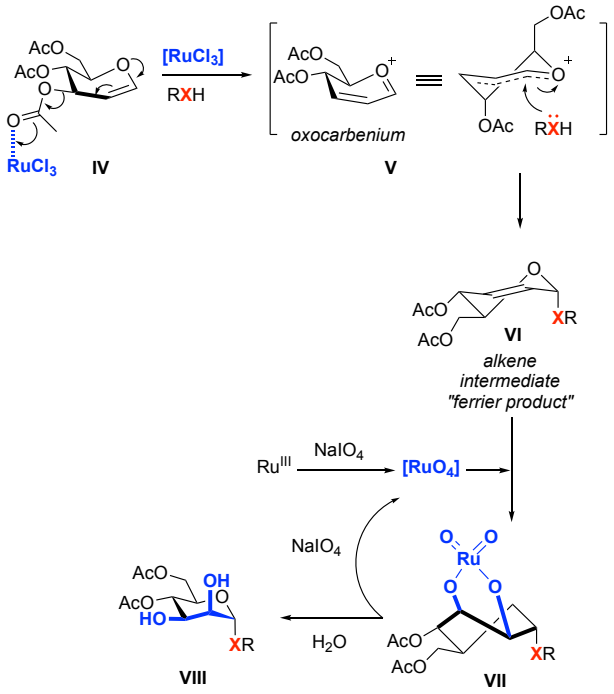

Scheme 9. Proposed mechanism for $RuCl_3$-catalyzed sequential glycosylation-dihydroxylation.

2.3. Application in synthesis

The $RuCl_3/NaIO_4$ protocol is now commonly used as classic method in multistep synthesis. For example in the total synthesis of the lactonamycin a key step involves a *syn*-hydroxylation of electron-poor C=C bond of an antraquinone motif.[29] The reaction using Shing's modified conditions generate the desired *syn*-diol **9** in good yield (71%, Scheme 9).[18a]

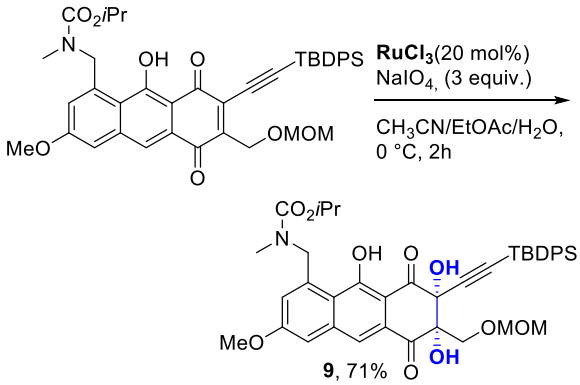

Scheme 10. *syn*-dihydroxylation step of the lactonamycin synthesis [29]

The synthesis of the C94–C104 fragment of the symbiodinolide, which is a marine natural polyol, has been achieved through a key $RuCl_3/NaIO_4$-catalyzed *syn*-dihydroxylation step (Scheme 11).[30] In this case the Plietker's conditions was not that efficient and the $CeCl_3$ was replaced by $ZnCl_2$ as a Lewis acid. Finally, the *syn*-dihydroxylated product **10** was obtained in 73% yield from the electron-poor enone. The *cis* relationship between the two newly formed hydroxyl groups was unambiguously assigned by NOESY experiment. It is noteworthy that with OsO_4 no dihydroxylation occurred.

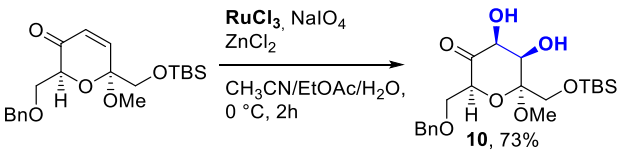

Scheme 11. *Syn*-dihydroxylation step of the synthesis of the C94-C104 fragment of symbiodinolide . [30]

Iida and co-workers described the synthesis of oxysterols which are atypical precursors of cholesterol derivatives.[31] The crucial step involved a *cis*-4α,5α-dihydroxylation of the allylic 3β-acetoxy-Δ^4 intermediate **11** (Scheme 12). Under the Plietker's condition the desired *syn*-diol was obtained quickly in good yield (72%). Here also, the OsO_4 or $KMnO_4$ were found ineffective as oxidant.

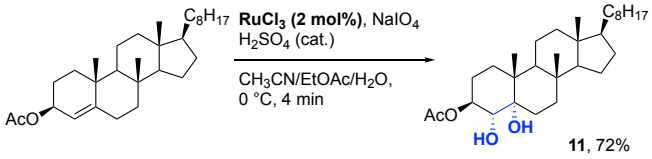

Scheme 12. *Syn*-dihydroxylation of cholest-4-en-3β-yl acetate. [31]

Allais and his colleague described the synthesis of D-(+)-ribono-1,4-lactone, a versatile chiral sugar synthon for the synthesis of natural products from (*S*)-γ-hydroxymethyl-α,β-butenolide (HBO, Scheme 13).[20e] In their synthetic strategy, *syn*-dihydroxylation was the key step. Even if in this case the modified Upjohn-type protocol gave higher yield than the ruthenium system, this later yielded the *syn*-diols **12-14** with high selectivity (up to 97/3).

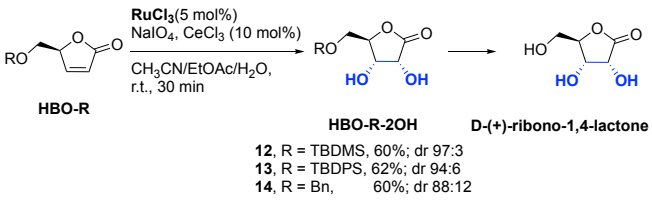

Scheme 13. *Syn*-dihydroxylation of HBO-R. [20e]

2.4. Well-defined Ru complexes

Che and co-workers were the first to report the use of well-defined ruthenium-oxo complexes surrounded by auxiliary ligands to modulate the reactivity of the active ruthenium(VI) center.[32] The ligand 1,4,7-trimethyl-1,4,7-triazacyclononane ligand (Me_3tacn) was combined to a Ru center to form the desired $[(Me_3tacn)(CF_3CO_2)Ru^{VI}O_2]ClO_4$ complex **A** (Figure 3). The ruthenium complex reacted stoichiometrically with a diverse array of alkenes in aqueous *tert*-butyl alcohol to give the corresponding *syn*-1,2-diols usually in excellent yield (Scheme 14a-b). The authors display important features: (i) the reaction media was found crucial as use of acetonitrile as solvent completely reversed the selectivity of the reaction in favor of the double bond cleavage and (ii) the formation of *syn*-diols was observed with the two *oxo* ligands being in *cis* position.

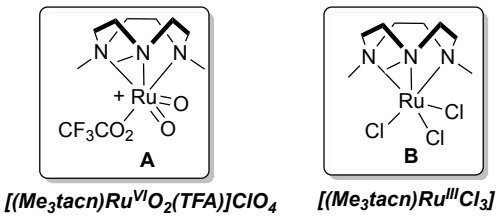

Figure 3. Well defined Ru(tacn) complexes used in *syn*-dihydroxylation.

Later on, the same author reported a catalytic version of this reaction in presence of only 1 mol% of the chloride complex **B** (Figure 3).[33] The system requires the presence of an oxidant such as H_2O_2 and a mixture of Al_2O_3/NaCl as additive was found beneficial for the *syn*-diol selectivity. Good yields from various non-functionalized cyclic, and styrenic alkenes were obtained (70-96%, Scheme 14c-d). However, even though the terminal and internal alkenes were oxidized to the corresponding *cis*-diols up to 96%, lower substrate conversions were observed (80-60%).

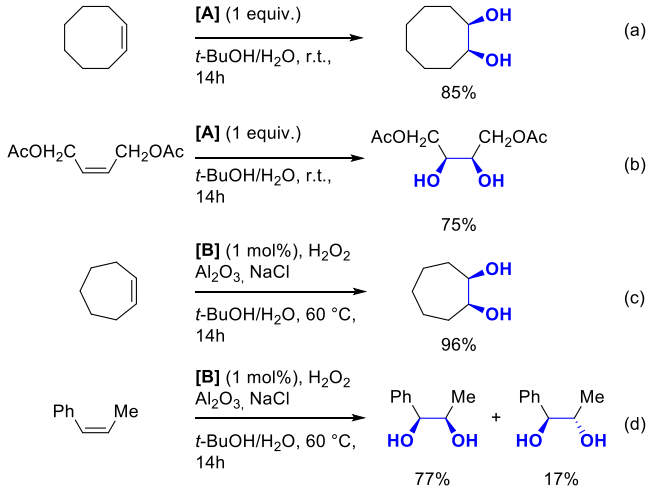

Scheme 14. *Syn*-dihydroxylation of alkene catalysed by $[(Me_3tacn)(CF_3CO_2)Ru^{VI}O_2]ClO_4$ **A** or $[(Me_3tacn)Ru^{III}Cl_3]$ **B** (Reaction time 14h).[32-33]

So far, studies on highly oxidizing well defined *cis*-dioxoruthenium(VI) complexes have focused only on tridentate Me_3tacn however such ligand displays very limited flexibility for structure modification. To overcome such issue, 'N_4'-ligands have been used; their higher rigidity and denticity would provide better conformational stability under catalytic conditions. Che *et al.* have recently proposed various chiral N_4 ligands which combine one diamino and two pyridine fragments to envelop the ruthenium center (Figure 4).[34]

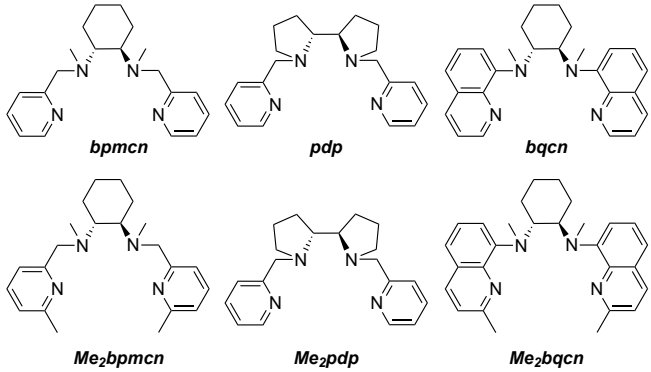

Figure 4. N_4 polydentate chiral ligand. [33]

By mixing the desired ligand with a ruthenium source, *cis*-$[(N_4)Ru^{III}Cl_2]^+$ complexes were easily *in-situ* generated. X-ray spectroscopy analyses on these complexes showed the strong preference for the formation of the *cis*-α dioxo configuration. Remarkably the authors isolated the ruthenium-oxo complex *cis*-$[(bpmcn)Ru^{VI}(O)_2]^{2+}$ **D** by simple treatment of *cis*-$[(bpmcn)O_2CCF_3$ **C** with excess CAN (cerium ammonium nitrate)

in aqueous solution (Figure 5). Electrochemical analyses showed that the chemically/electrochemically generated *cis*-$[(bpmcn)Ru^{VI}(O)_2]^{2+}$ **D** was a pretty strong oxidant (E^o = 1.11–1.13 V vs. SCE at pH 1).[34]

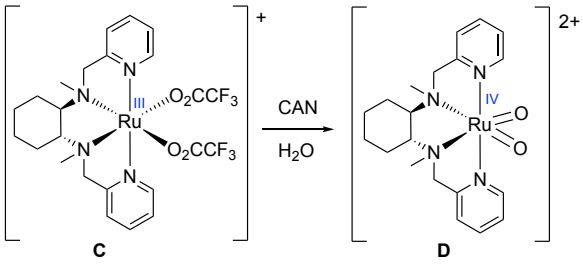

Figure 5. Synthesis of *cis*-$[(bpmcn)Ru^{VI}(O)_2]^{2+}$complex (**D**).

Complex **D** was then further evaluated stoichiometrically in the *syn*-dihydroxylation of several olefins. In most cases, the oxidation afforded ca. 1:1 mixture between diols (*syn* and *anti*) and aldehydes. When using a chiral (*R,R*)-bpmcn, only poor enantiomeric excess (ranging from 24 to 36%) were observed for both the *syn*- and *anti*-diols (Scheme 15a-b). According to the authors, the *syn*/*anti* mixture obtained for diols may indicates the non-concerted nature of the dihydroxylation reaction. However this represents the only example of chirality-induced by the ligand, the other rare example of RuO_4-mediated asymmetric dihydroxylations are all based on a stoichiometric chiral auxiliary approach in which the alkenes substrates carry the chiral auxiliary.[20b, 23, 35]

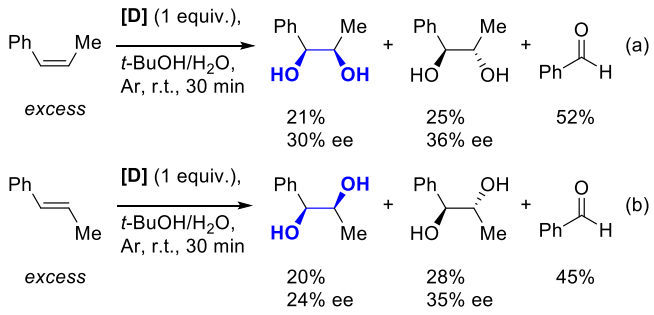

Scheme 15. *Syn*-dihydroxylation reaction with ruthenium catalyst **D**. [33]

3. Manganese-mediated *syn*-dihydroxylation

As the cheapest and least toxic alternative to osmium, the permanganate ion has been widely used and studied for the *syn*-dihydroxylation of olefins since the first report by Kekulé and Anschütz over a century ago.[36] Since that time, many reagents based on manganese have been developed and successfully used under alkaline condition, however the yields are rarely as high as those obtained with OsO_4. Three main strategies have emerged which use (i) homogenous conditions for $KMnO_4$ (or tetraalkylammonium-MnO_4) (ii) heterogeneous conditions in presence of a phase-transfer catalyst and (iii) well-defined Mn-catalyst in presence of an oxidant under homogeneous conditions.

The conventional potassium permanganate, due to its low solubility in organic solvents, is generally used in the form of its aqueous solution, however lower yields caused by overoxidation in the aqueous phase are often observed. Furthermore, the range of suitable substrates is restricted to those soluble in water (Scheme 16). This is why many efforts have been devoted to the second and third approach by the scientific community.

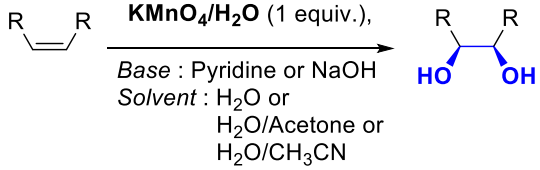

Scheme 16. Standard conditions using aqueous MnO_4.

Since, the literature covering *syn*-dihydroxylation with permanganate reagents is very rich,[37][38] only the latest examples of its use will be highlighted here.

3.1. Homogenous system using co-oxidant.

$KMnO_4$ was generally used in more than one equivalent which often leads to the formation of overoxidized products. In order to address this issue, the Gültekin's group used H_2O_2 (3 equiv.) as co-oxidant which allowed them to decrease the amount of permanganate to 0.5 equivalent without loss of activity (Scheme 17).[39] Consequently the dihydroxylation of several olefins was performed with $KMnO_4$, hydrogen peroxide in a water–acetone mixture (1:2) at 0 °C under nitrogen to provide *syn*-diols in 2 hours and in good yield (60-95%). It is known that during the course of the oxidation reaction with $KMnO_4$ that various manganese oxide derivatives could be formed. Careful spectroscopic analyses (TEM, SEM, XPS, XRD and EDX) of the solid residue obtained at the end of the reaction showed that the manganese aggregate was mainly composed by Mn_3O_4. To better understand the role of such manganese species, a test was performed with commercial Mn_3O_4 in the presence of H_2O_2. The results show that 34% of diol was produced along with the degradation products, which indicates that this manganese species plays a major role in the oxidation reaction.

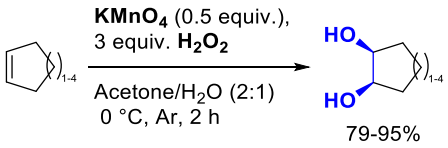

Scheme 17. *Syn*-dihydroxylation reaction with $KMnO_4/H_2O_2$ system. [39]

3.2. Heterogeneous system using phase-transfer catalysts.

3.2.1. Ammonium based-PTC:

To improve the efficiency of $KMnO_4$ and also increase the variety of usable olefin substrates, a phase transfer catalyst

(PTC), most often a quaternary ammonium salt, can be used.[8] The first used was the benzyltriethylammonium chloride (TEBACl) in a dichloromethane/water system which gave only moderate yields. Subsequent to this discovery many different PTCs were evaluated such as cetyltrimethylammonium, triethylbenzylammonium, tetradecyltrimethylammonium, dicyclohexyl-18-crown-6 and many others.[40] Solid-liquid phase transfer is also possible under non-aqueous conditions.

Recently, Luo *et al.* reported a new and improved non-aqueous protocol for the *cis*-dihydroxylation of acrylate derivatives.[41] Using 1.2 equiv. of benzyl(triethyl)ammonium chloride (TEBACl) in acetone at 0 °C, *syn*-diols were produced in high yield (78-96%) and no overoxidation products were observed (Scheme 18). However, unfunctionalized olefins didn't give better yields than those obtained in the absence of TEBACl and the cinnamate substrates were almost non-reactive. The reaction could be scale up to 190 g of $KMnO_4$ without any loss of activity or selectivity giving 211 g of the desired diol (scheme 18c).

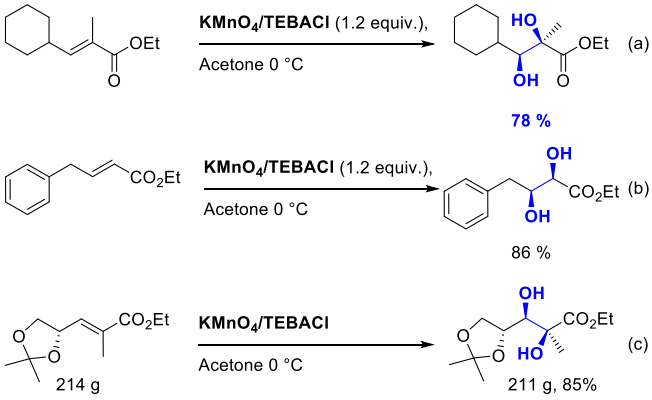

Scheme 17. *Syn*-dihydroxylation of acrylate derivatives with TEBAC/$KMnO_4$.[41]

Later the same author improved the system by using only 10 mol% of a lipophilic imidazolium salt instead of TEBACl (Figure 6).[42] According to the author, the two dodecyl chains attached to the nitrogen atom of imidazolium could increase the solubility of the permanganate species and the diol products were obtained with a good yield without any trace of secondary oxidized products.

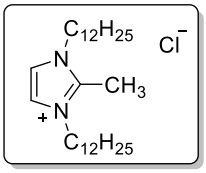

Figure 6. Phase transfer catalyst imidazolium type used in *syn*-dihydroxylation. [42]

3.2.2. Chiral version of ammonium based-PTC

An asymmetric version of this PTC-strategy was first reported by Brown which used a stoichiometric amount of a *Cinchonidinium* salt.[43] Unfortunately the low stability of this ammonium salt under the oxidation conditions leads to moderate enantioselectivities

In 2015, Tan and co-workers applied this PTC concept through the development of chiral cation-controlled ion-paring catalysis.[44] They disclosed that chiral dicationic bisguanidinium **BG** is stable under the oxidation conditions and is recoverable at the end of the reaction (Scheme 19). The authors suggested that rate acceleration is mainly assigned to transition state stabilization through attractive cation−anion interaction which favored the asymmetric pathway. Using 2.0 mol % of (*S,S*)-**BG**, 20 wt % aqueous potassium iodide (KI), 1.5 equiv. of $KMnO_4$ in *tert*-butyl methyl ether (TBME) at low temperature (-60 °C), the oxidation of the α,β-unsaturated ester proceeded smoothly to afford diol in moderate yield (60-72%) but with excellent enantioselectivity (84-96% ee, Scheme 19a-b). However significant amount of C-C cleavage product was observed in all cases. Substrates carrying electron-rich aryl groups mainly lead to higher enantioselectivities than those deficient in electrons. However, even if the substrates of trisubstituted enoates (Z / E mixture) generate diols with a high enantioselectivity, this reaction mainly produced the C-C cleavage product. Finally under acidic media, the C-C cleavage was suppressed however one of the hydroxy groups is converted into ketone generating the 2-hydroxy-3-oxocarboxylic ester as the sole product of the reaction in good to moderate yield and high enantioselectivities (up to 96%, scheme 19c. Interestingly, in this case, the *Z*- and *E*-olefins were transformed into the same enantiomer.

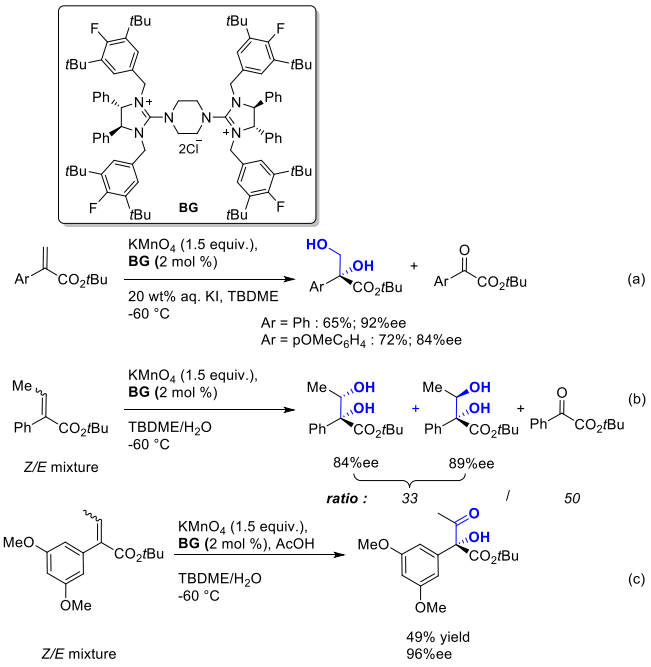

Scheme 19. Asymmetric permanganate dihydroxylation in in presence of chiral dicationic bisguanidinium **BG**. [44]

3.3. Well-defined Mn complexes.

3.3.1. Manganese trimethyl-triazacyclononane based ligands

The first example of manganese-catalyzed dihydroxylation was reported by Vos *et al.* using a Mn surrounded by *N,N',N''*-

trimethyl-1,4,7-triazacyclononane (tmtacn) ligand and attached on solid support with H_2O_2 as a reoxidant.[45] Following this seminal report, several groups (De Vos, Feringa) investigated further the use of well-defined Mn(tmtacn) complexes (Figure 7).[46] Several additives have been evaluated in order to increase the selectivity of the diols with respect to the epoxides. These studies demonstrated that in presence of a carboxylic acid in particular the *syn*-dihydroxylation was highly favoured and the reactivity doped. The role of the acid is double; first it serves to protonate the manganese species to facilitate is reduction by H_2O_2 to Mn^{III} and Mn^{II} species and secondly it acts as bridging ligand between the two Mn atoms stabilizing this complex. Variation in the carboxylic backbone shows two important features: (i) the greater the electron deficiency of the carboxyl group, the more the activity is increased, (ii) the selectivity is dictated by the steric bulk of the 2,6-position of benzoic acids.[46c] With such system Feringa and his colleagues reach over 8000 turnovers to the *cis*-diol product from electron-rich *cis*-olefins, but this system is poorly active with electron deficient alkenes [46b-e]

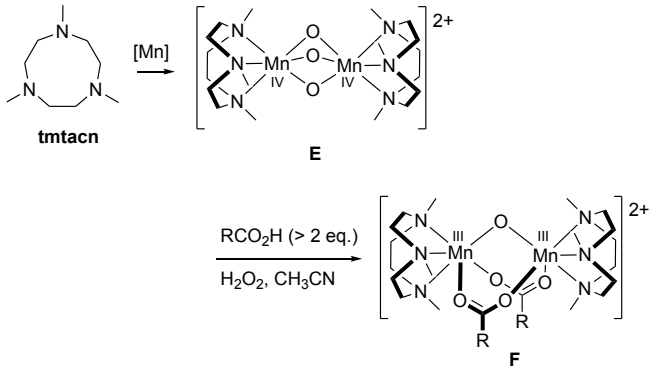

Figure 7. Well defined Ru(tacn) complexes. [46]

Notestein and co-workers[47] reported a heterogeneous catalyst by grafting the Mn(tmtacn) complex onto mesoporous silica (Figure 8). The immobilization of the manganese catalyst occurs by *in situ* reduction of $[(tmtacn)Mn^{IV}(\mu\text{-}O)_3Mn^{IV}(tmtacn)]^{2+}$ in the presence of silica particles coated with carboxylic acid. Then addition of H_2O_2 generates the active grafted $[(tmtacn)Mn^{III}(\mu\text{-}O)(\mu\text{-}RCOO)_2Mn^{III}(tmtacn)]^{2+}$ species.[48] Careful spectroscopic analyses confirmed that the Mn^{III}/Mn^{III} dimer was fixed onto the acid-functionalized silica surface. This *in situ* anchored catalyst was then evaluated in the oxidation of cyclooctene. The same level of activity as of the homogenous system was observed.[46c] Curiously, the amount of valeric acid attached to SiO_2 has a significant positive impact on the total turnover compared to the same soluble amount (factor of 9). Finally, the mechanism of this system was studied by computational analyses and microkinetic modelling which concluded that the rate determining step was the activation of the complex with H_2O_2.[47d]

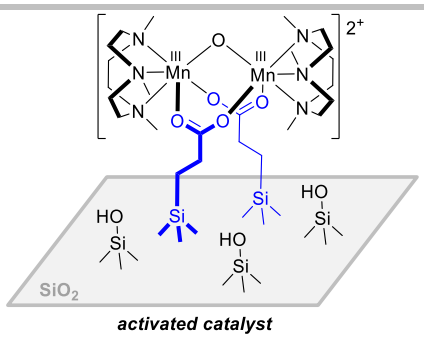

Figure 8. Active catalyst grafted on acid functionalized-SiO_2. [47]

3.3.2. Manganese pyridine-2-carboxylic based ligands

Inspired by mechanistic studies on the decomposition of polypyridylamine-based manganese catalysts (Scheme 20), a highly efficient system for *cis*-dihydroxylation of electron-poor alkenes has been developed (Scheme 21a-b).[49] The catalytic species is composed of pyridine-2-carboxylic acid (PCA) as ligand in presence of H_2O_2, a base (NaOAc), appropriate ketone and $Mn^{II}(ClO_4)_2$. In this case, the active species is always generated *in situ*. By contrast under the same catalytic conditions, electron-rich alkenes promote the formation of epoxides with good selectivities.[46f]

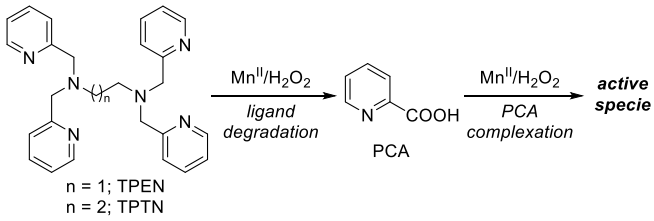

Scheme 20. Oxidative decomposition of polypyridyl ligands to pyridine-2-carboxylic acid (PCA). [49]

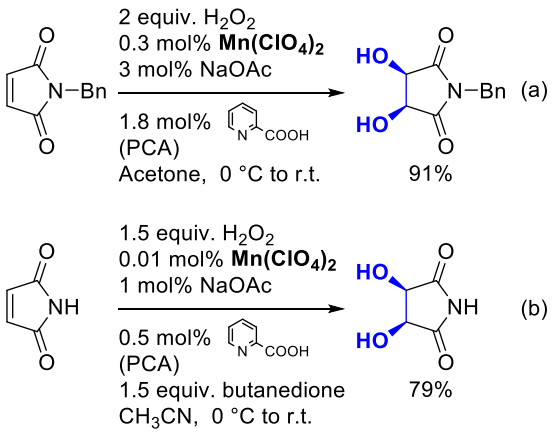

Scheme 21. PCA/Mn-catalyzed *syn*-dihydroxylation of electron-poor olefins. [50]

This PCA system was improved by Browne and co-workers to avoid the use of potentially explosive combination of acetone/H_2O_2 by using a slight excess of butanedione (1.5

equiv.) in acetonitrile.[50] Importantly, this system enables extremely low catalyst loadings (<0.01 mol %). Here the role of the ketone is to form a hydroperoxide adduct which was demonstrated to be the active oxidant of the reaction. This reaction is reversible and the formation of ketone-peroxide adducts was identified by Raman spectroscopy (Scheme 22).[51] Here again, only electron poor alkenes are able to selectively give *syn*-diol products (Scheme 21b). Mechanistic investigations indicate that the rate determining step is the formation of the active oxidizing species by reaction of 3-hydroperoxy-3-hydroxybutanone with the manganese catalyst (Figure 9).[51-52] In addition, even if its role remains undefined, the acetic acid formed by this mechanism is crucial to achieve a significant oxidation rate.

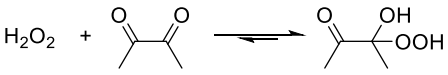

Scheme 22. Equilibrium between butanedione/hydrogen peroxide and 3-hydroperoxy-3-hydroxybutanone.

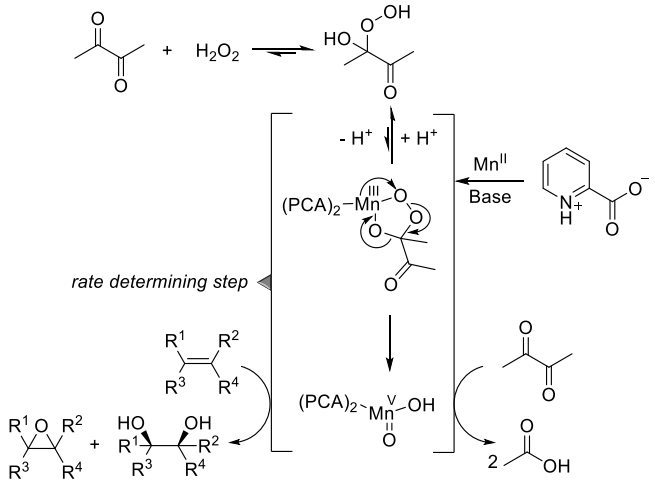

Figure 9. Proposed Mechanism for the Oxidation of Alkenes under a PCA/Mn catalytic system. [51-52]

3.3.3. Asymmetric dihydroxylation

Although the first asymmetrical example was described almost 20 years ago by Brown *et al.*,[43] only a few reports have been published since then.[7b, 53] Feringa and coworkers combined the $[Mn^{IV}_2(\mu\text{-}O)_3(tmtacn)_2]^{2+}$ complex with enantiopure carboxylic acids to induce asymmetric induction using H_2O_2 as oxidant (Figure 10).[46e] The evaluation of more than 24 different additives revealed that acetyl protected D-phenylglycine was the best candidate, generating the corresponding *cis*-diol from 2,2-dimethyl chromene substrate with a high conversion and moderate enantioselectivity (54% ee) but yet promising.

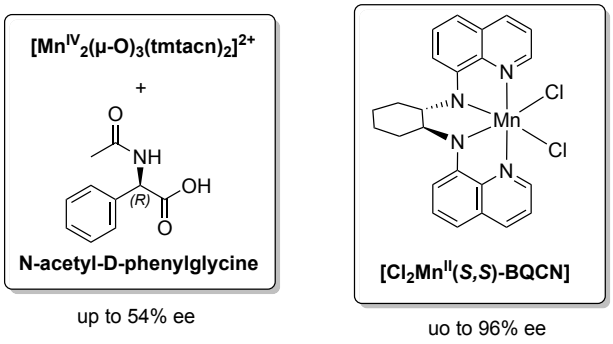

Figure 10. Example of chiral catalytic systems for *cis*-dihydroxylation based on Mn.

Shortly after, Che and co-workers displayed the involvement of unprecedented *cis*-$Mn^{V}(O)_2$ species in asymmetric *cis*-dihydroxylation of electron-deficient olefins with Oxone and catalyzed by a chiral Mn^{II} complex.[54] The tetradentate ligand N_4-donor (*S,S*-BQCN) is built around a chiral diaminocyclohexane motif which generates the *syn*-diols in high yield and with up to 96% ee (Figure 10) . It is Noteworthy that electron-poor olefins are still prone to form significant amount of epoxides (8-30%, Scheme 23). The situation is even worse for electron-rich olefins which generate a nearly 1: 1 mixture of epoxide and *syn*-diol. For terminal olefins, such as styrene and benzyl acrylate, lower ee's have been observed (24% and 47%, respectively). Interestingly, the reaction could be scale up to 2 grams of substrate without any change in the level of the enantiomeric induction.

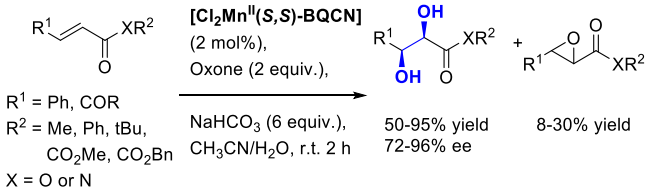

Scheme 23. Oxidation of alkenes with Oxone catalyzed by Mn(*S,S*)-BQCN.[54]

4. Nonheme Iron mediated *syn*-dihydroxylation

Living organisms, thanks to their enzymes, are able to oxidize non-trivial substrates which contain demanding C = C and C-H bonds using iron capable of activating O_2 or H_2O_2.[55] Numerous investigations have been devoted to the development of biomimetic models of cytochrome P450 and related enzymes *via* the synthesis of iron-porphyrin complexes.[56] However, simpler and less synthetically demanding ligands are necessary for large-scale industrial processes.

Interestingly, Rieske dioxygenases, an important class of non-heme iron enzyme, react with olefinic substrates with high levels of chemo-, regio- and stereoselectivity. The capacity of these enzymes to promote the selective and asymmetric *syn*-dihydroxylation of double bonds is of particular interest. It makes it a subject of major interest among chemists and biochemists. Therefore, bio-inspired nonheme iron catalysis has been studied and developed intensively particularly over the past 10 years, showing great potential for such transformations (racemic and

asymmetric).[57] Finally, combined with their selectivity and to the fact that iron is one of the most abundant metals on earth, it makes the development of such complexes very attractive for future sustainable economic growth. Several excellent reviews covering non-heme iron oxidation reactions have been recently published,[7b, 53, 58] therefore we will only focus on the most remarkable results of the last decade.

The first example was reported by Que *et al.* in the early 2000s, in which a polydentate N_4-donor ligand was used to form a [Fe(II)(tpa)] complex which catalyzed oxidative transformations in presence of H_2O_2 as oxidant (TPA = Tris(2-Pyridylmethyl)Amine) (Figure 11) .[59]

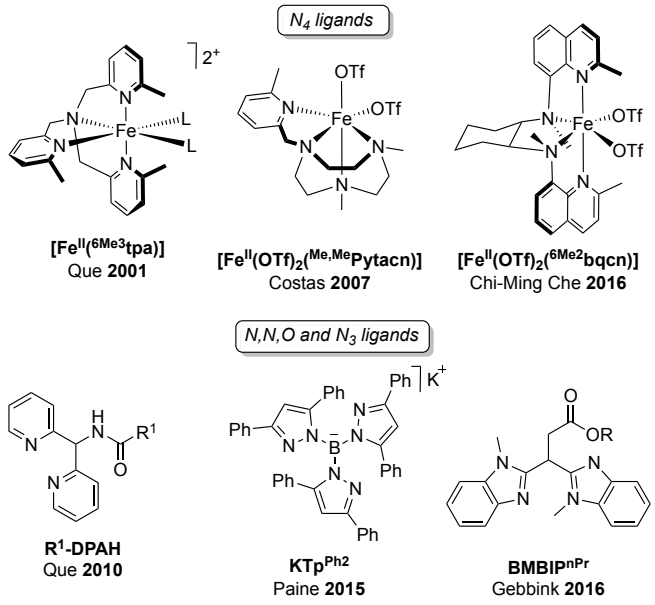

Figure 11. Molecular structure of representative ligands and iron complexes structures for *syn*-dihydroxylation

Several groups have rapidly extended this chemistry by developing different ligand backbones with nitrogen-containing Lewis bases. However, other ligands which incorporate donor N,O atoms or which have a N,N,O tripod backbone also exhibit excellent chemoselectivity for *syn*-dihydroxylation.[60] Anyway, all these catalysts have in common important feature[7b, 53, 58] such as : (i) they are mainly tetradentate and are based on aminopyridine ligand, (ii) they possess two labile coordination sites with a *cis*-relationship which is necessary to be both accessible for the coordination and activation of the peroxide, (iii) the ligands have to favor high-spin iron metal centers, (iv) the introduction of the methyl group in the 6th position of the pyridine ring is required because it allows a significant steric repulsion with the iron atom, which prevents the formation of shorter Fe-N bonds necessary for the low spin state, (v) the topology of N_2Py_2-complexes is also a key variable. Indeed, the *cis*-α topological configuration is much more favorable for *syn*-dihydroxylation than that of *cis*-β while the *trans* topology gives rise to inactive oxidation catalysts (Figure 12).[61] Finally (vi) most often, the hydrogen peroxide is used as the oxidant of choice.

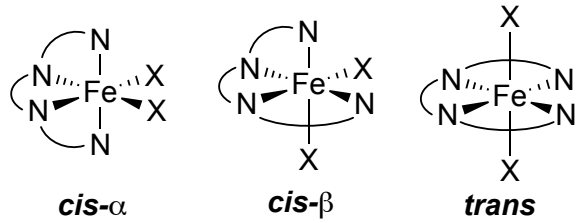

Figure 12 Topological isomers for N_4 ligands in an octahedral geometry.

4.1. H_2O_2 activation

4.1.1. Mechanistic consideration

Extensive mechanistic studies have shown that non-heme iron catalysts can be divided into two distinct classes, usually called class **A** and class **B** as displayed in Figure 13.[58c, 62]

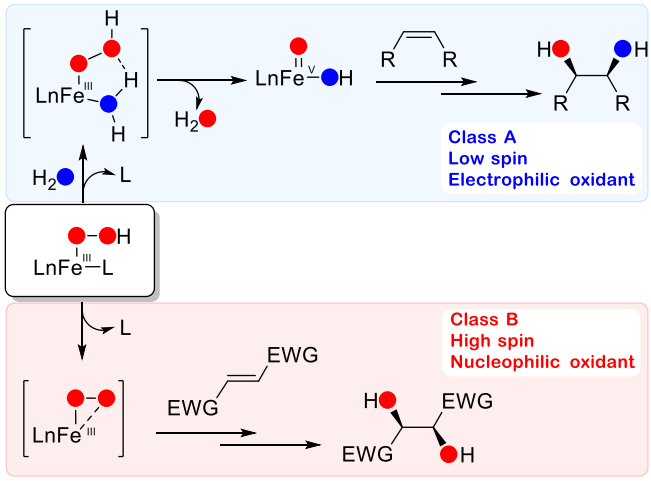

Figure 13. Two distinct models : class **A** and class **B** catalysts.

Class **A** catalysts produce a low spin Fe^{III}-OOH intermediate which generates, *via* the heterolysis of the O-O bond, the active $Fe^{V}(O)(OH)$ electrophilic species. Theoretical calculations onto (tpa)- and (^{Me,H}Pytacn)-Fe^{V}-oxo complexes indicate that the hydroxyl, linked to Fe^{V}, attacks the olefin first.[63] In contrast, class **B** catalysts form an oxidizing species which has a nucleophilic character. In this case, the transfer of oxygen on the double bonds is carried out by a high spin $Fe^{III}(OOH)$ species *via* a concerted mechanism by simultaneous rupture of the O-O bond as shown by DFT calculation for complex [Fe(OTf)$_2$(^{6Me2}bqcn)] (Figure 11).[64] This underlines the importance of controlling the spin state of the peroxido-iron intermediate to obtain high *syn*-diol selectivity by reacting it with appropriates electron-poor or electron-rich alkene.[65] A water-assisted mechanism has been proposed for class **A** on the basis of experiments with labelled $H_2{}^{18}O$.[58c, 62] These results showed that the *cis*-diol product incorporates an oxygen atom from H_2O_2 and the other from H_2O which involves an oxidation mechanism consisting of an O atom of each of these molecules. However, for class **B** the two oxygen atoms of a single $H_2{}^{18}O_2$ molecule are incorporated into the corresponding *syn*-diol which indicates a non-water-assisted mechanism.[58]

4.1.2. Recent advances in H_2O_2-mediated oxidation

In the quest to reduce the amount of alkene substrate, often used in large excess, Beller and Costas investigated the effects of the aromatic substitution pattern onto the pyridine rings of the PyTACN ligands (Figure 14).[66]

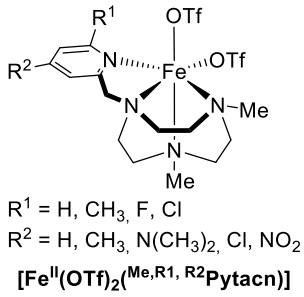

Figure 14. Molecular structure of [Fe(II)(^{Me,R1,R2}PyTACN)(CF_3SO_3)$_2$] complexes.[66]

In this study both the electronic and steric effect respectively at the position 4 and 6 of the pyridine were explored (Figure 14). Mixture of *syn*-diol and epoxide products were obtained under smooth conditions which use large excess of *cis*-cyclooctene (1 equiv.), reduced amount of H_2O_2 (10-100 milliequivalent) and 0.1 mol% with iron catalyst. Substitution at position 4 of pyridine only shows slight *cis*-dihydroxylation selectivity at low concentration of H_2O_2, suggesting a minor influence of electronic effects, while selectivity is lost at higher peroxide concentrations resulting in almost equimolar mixtures of epoxide and diol. The bulky groups in the 6-position, have a much stronger chemoselective impact towards *cis*-dihydroxylation giving for the complex [Fe(OTf)$_2$(^{Me,Me,H}PyTACN)] a diol / epoxide ratio around 6/1. Attempts to use olefin as the limiting reagent (1 equivalent) in presence of 3 mol% of Fe catalyst and 2 equivalents of H_2O_2 produced the epoxide as the main oxidation product (diol/epoxide = 0.6). Fortunately, this selectivity can be completely reversed by the addition of 15 equivalents of water (diol/epoxide = 3.6). Best results were obtained with terminal or *cis*-aliphatic olefins for which the *syn*-diol product was obtained in 25–56% yield with a diol/epoxide ratio ranging from 1.8 to 3.6 (Scheme 24). *Trans* and aromatic alkenes were not suitable for this method because they generated mostly epoxides and overoxidation products, respectively. In addition, electron-poor olefins such as diester dimethyl fumarate remained unreactive under these oxidation conditions. This catalytic discrimination was successfully applied to (*2E,6Z*)-nona-2,6-dienyl acetate substrates in which only the *cis*-double bond was oxidized (scheme 24c). A time course analysis of the reaction, without and in the presence of *cis*-diol at the start of the reaction was conducted. This study has shown that at high diol concentrations, the epoxidation and overoxidation reactions are favored in place of the desired *syn*-dihydroxylation. According to the authors, the *syn*-diol products could bind reversibly to the iron site and thus poison or slow down the catalyst and that the crucial role water was to help the release of the diol from the ferric glycolate species.

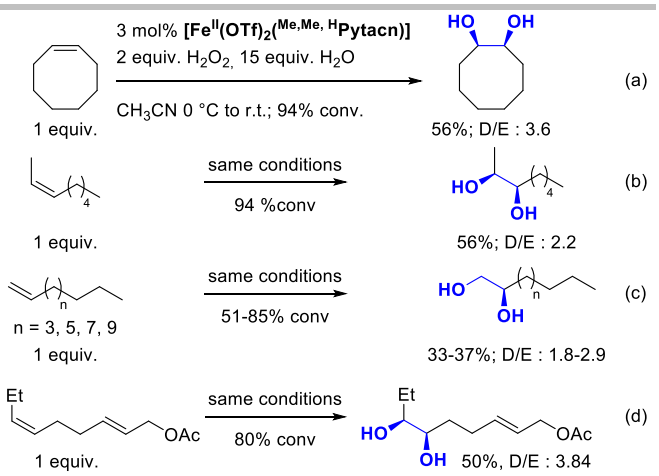

Scheme 24. *Syn*-hydroxylation catalysed by [Fe(^{Me,Me,H}PyTACN)(CF_3SO_3)$_2$].[66]

The catalyst was also able to oxidize unsaturated fatty esters giving the *cis*-diol with both moderate yield and selectivity (diol/epoxide = 1.8); however addition of water was found detrimental due to solubility issue.[67] Of note, Gebbink and co-workers also obtained an X-ray structure of [Fe(OTf)$_2$(^{Me,Me,H}PyTACN)] complex which shows elongated Fe-N bonds (Fe-N_{Pyr} 2.246 Å and FeN_{amine} between 2.199-2.238 Å) indicative of a high spin ferrous center. [67]

4.1.3. Influence of additives to the selectivity

The addition of acetic acid has been shown to be detrimental to the production of diol and the selectivity was strongly shifted towards the formation of epoxide even if the [Fe^{II}(BQCN)] and [Fe^{II}(BPMCN)] complexes have the correct topology (Figures 3 & 11). Indeed, for *cis*-β isomer complexes, the presence of acetic acid changes the nature of the oxidant from being nucleophilic (class **B**) and *cis*-diol-selective to electrophilic and epoxide-selective. In addition, this new catalytic system is now more suitable to now prefers to oxidize electron-rich olefins rather of electron poor substrates (Scheme 25).[68] Such reactivity modulated by the addition of simple additive such as H_2O and AcOH opens interesting perspectives on the control of the selectivity of the oxidation reaction.

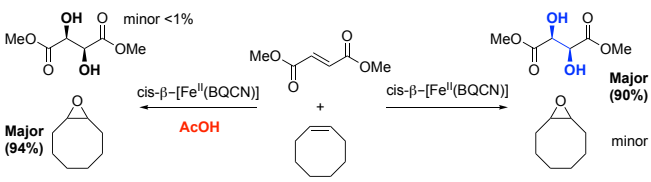

Scheme 25. Competition experiments for the oxidation of olefin pairs.[68]

Bandyopadhyay and co-workers described the synthesis and the use of (*μ*-oxo)(*μ*-hydroxo)diiron(III) complex based **G** on the amino pyridyl ligand bpmen [bpmen = *N,N'*-dimethyl-*N,N'*-bis(2-pyridylmethyl)ethane-1,2-diamine] with hydrogen peroxide under the conditions of limiting substrate (Scheme 26).[69] Using very smooth experimental conditions at room temperature (catalyst : substrate : HOAc : H_2O_2 = 1 : 20 : 1: 30), this catalytic system

showed high epoxidation selectivity for electron-rich olefins and high selectivity for *cis*-dihydroxylation for electron-deficient olefins (Scheme 26). For the electron deficient alkenes, the addition of acetic acid, prior the addition of the substrate, did not affect the formation of *cis*-diol and a modest improvement in the conversion of the substrate was observed but the yield remained moderate.

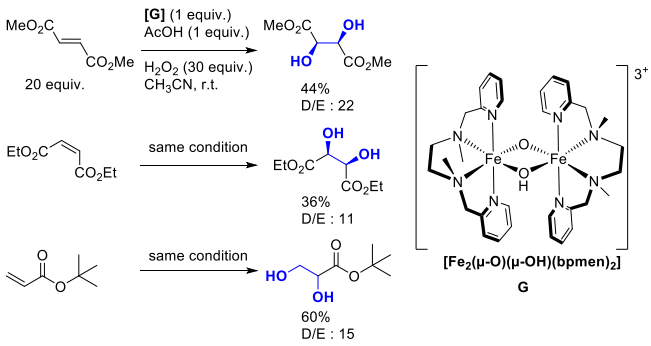

Scheme 26. *Syn*-dihydroxylation of electron-poor olefin by $[Fe_2(\mu\text{-}O)(\mu\text{-}OH)(bpmen)_2]$ catalyst. [69]

Among the very rare systems that operate under substrate-limiting conditions,[59c, 64, 66, 70] a major breakthrough has been recently disclosed by Costas and co-workers.[71] To overcome the deactivation of the catalyst during the reaction caused by the strong affinity of the diol generated over time, the authors proposed to control the release of the product which is a critical step. For this, they used two complementary strategies: first a more sterically demanding triisopropylsilyl (tips) groups has been introduced in position 5 of a pyridine rings of a tpa ligand, in order to increase the chemoselectivity and also limit the formation of non-active thermodynamic oxo-bridged diferric species. Secondly, a Lewis acid $[Mg(ClO_4)_2{\cdot}6H_2O]$ was added to trap the diol from the reaction mixture and thereby prevent its coordination to the metal. Using mild reaction conditions (1 mol % catalyst, 1.5 equiv. of H_2O_2, 2.2 equiv. of $Mg(ClO_4)_2{\cdot}6H_2O$ and 1 equiv. of alkene), diols were obtained in good to high yield with elevated chemoselectivity (Scheme 27).

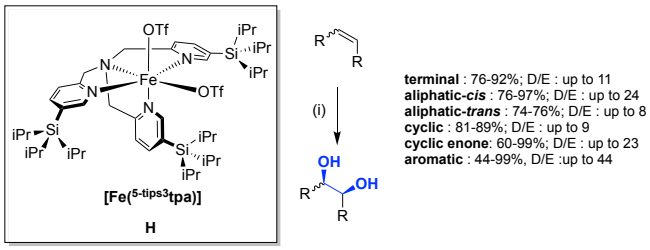

Scheme 27. *Syn*-dihydroxylation with sterically demanding Fe^{TIPS} complex. Reaction conditions: (i) 1 mol% [Fe] **H**, 1.5 equiv. H_2O_2, 2 equiv. $Mg(ClO_4)_2$, CH_3CN, 0 °C.[71]

The scope of the reaction is quite wide and the iron catalyst **H** was capable of oxidizing either aliphatic olefins (terminal, *trans*, *cis* and cyclic) as cyclic enones or even challenging aromatic olefins (deactivated and non-deactivated). Remarkably, this catalytic system is tolerant to several functional groups such as amide, alcohol, halide or ester. Interestingly also, electron-poor olefins are also transformed into *cis*-diol with good selectivity. In general, *cis*-olefins always generate better chemical yield than *trans*. However, too sterically demanding substrates reduce the efficiency of the reaction and olefins such as 2,3-dimethyl-3-butene are unreactive, suggesting sensitivity of the catalyst to steric substrate. Competitive experiments between poor and electron-rich olefins indicated that oxidizing species have a rather electrophilic character. The authors used these reactivity differences to selectively oxidize specific double bonds present into challenging substrates such as *cis/trans*-jasmine or steroidal derivatives (Scheme 28).

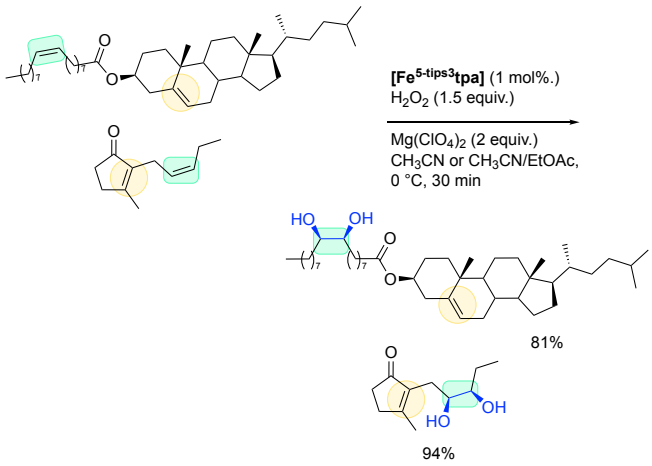

Scheme 28. Selective alkene oxidation.[71]

Isotopic labelling analysis confirmed the class **A** nature of the iron catalyst which produced the corresponding mono-^{18}O-labeled *syn*-diol in 90%.

Labelling experiments using $H_2{}^{18}O$ also showed that the incorporation of ^{18}O atom is regioselective and occurred at the less hindered carbon for the unsymmetrical olefins substrate. This was due to the unique different structural constraints of the two labile sites (O_A & O_B) which are induced by the bulky TIPS groups (Figure 15). These results strongly indicate that the oxygen atom from water occupies the O_A position while the hydrogen peroxide occupies the O_B position in the $[Fe^{V}(O)(OH)(^{5\text{-tips}3}tpa)]^{2+}$. The higher ratio between the two positions was observed for the vinylcyclohexane for which the terminal carbon atom was regioselectively ^{18}O-labeled with a 19:81 ratio (Figure 15). Compared with the bulky substitution in α position which increases the diol-selectivity in detriment to the reactivity, the substitution in β position makes it possible to preserve the integrity of the catalyst while keeping a high chemoselectivity for the diol product.

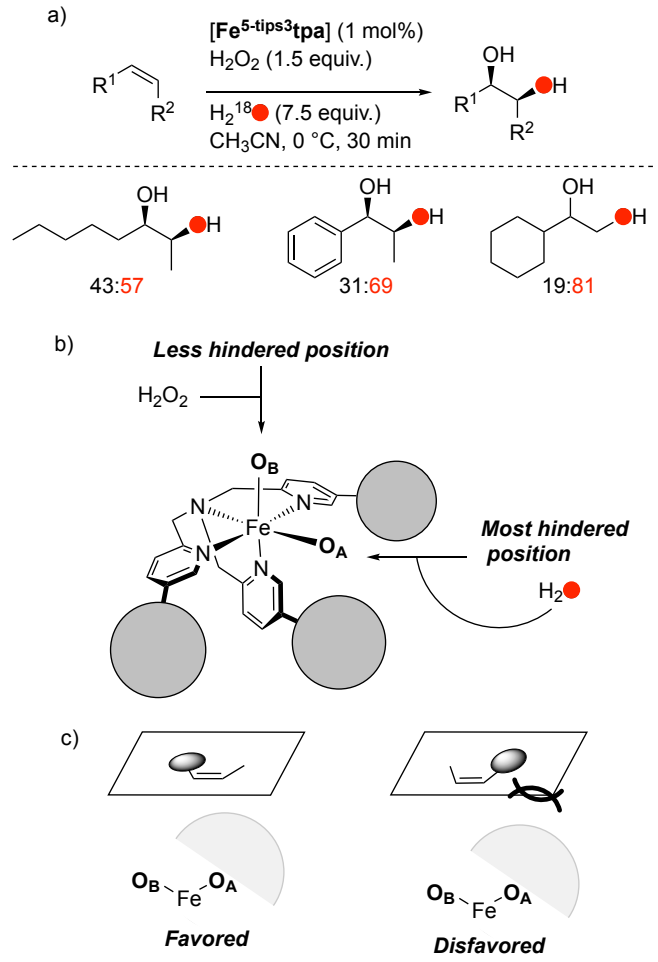

Figure 15. a) Isotopic labeling analysis. b) The proposed site of H_2O_2 and H_2O binding to the catalyst derived from the isotopic labeling study. c) Proposed model to rationalize the favored and disfavored approach of the olefin to the iron catalyst based on steric interactions. [71]

Lately, this system has been brought to greener considerations by eliminating acetonitrile to the benefit of a polypropylene carbonate/ethyl acetate mixture (PC/EtOAc 1/1) (Scheme 29).[72] Similar reactivity and selectivity have been obtained with catalyst $[Fe(^{5\text{-tips}3}tpa)]^{2+}$ using this mixture of solvents with respect to acetonitrile. The same trend was observed for the regioselectivity of the catalyst when two different olefinic sites are present in the same molecule, for which the attack occurs at the least hindered double bond. Interestingly the active species can be generated *in situ* by the combination of commercial and bench stable $[Fe(OTf)_2(CH_3CN)_2]$ and $^{5\text{-tips}3}$tpa ligand without loss of reactivity and selectivity. Once again addition of $Mg(ClO_4)_2{\cdot}6H_2O$ additive was necessary to significantly improve product yields and chemoselectivity of the reactions.

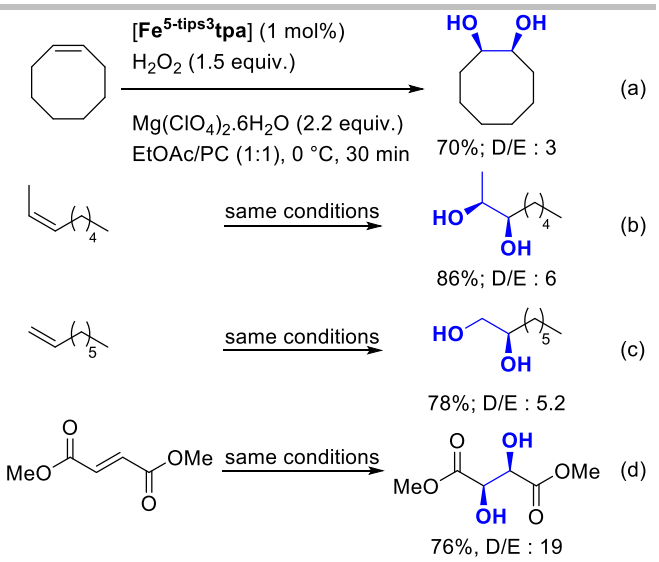

Scheme 29. Greener conditions for *syn*-hydroxylation reactions (PC = propylene carbonate). [72]

Well-defined Fe^{III} complexes such as $[Fe^{III}(Pc\text{-}L)(X)_2][X]$ complexes have been also used as precursor to generate the active Fe(III)-hydroperoxo species. Caselli and colleagues have shown that these $[Fe^{III}(Pc\text{-}L)(X)_2][X]$ complexes were able to generate cis-diols from alkene. (Scheme 30).[73] In this case the chemoselectivity of the reaction was strongly dependent on the nature of the anion that binds to the metal. The chloride complex $[Fe^{III}(Pc\text{-}L)(Cl)_2]Cl{\bullet}2H_2O$ favored the formation of the epoxide and shows a preference towards the formation of *trans* products to the exception of endocyclic compounds which provide majoritarily the diol compounds as depicted for the limonene (Scheme 30). In the other hands, when X = OTf, the resulting $[Fe^{III}(Pc\text{-}L)(OTf)_2][OTf]$ complex generated almost exclusively the acetal, arising from diol intermediates, as a *syn*/*anti* mixture. With the exception of a short range of endocyclic substrates, the formation of *trans*-acetonides was highly favored. Interestingly, under these conditions, limonene generated the diol instead of the expected acetonide product (Scheme 30). These results and selectivity might be explained by the fact that (i) in the presence of catalytic amounts of ferric Lewis acids and in acetone as solvent, epoxides could be readily converted into acetonides and (ii) and that a radical ring opening mechanism of epoxide could occur.

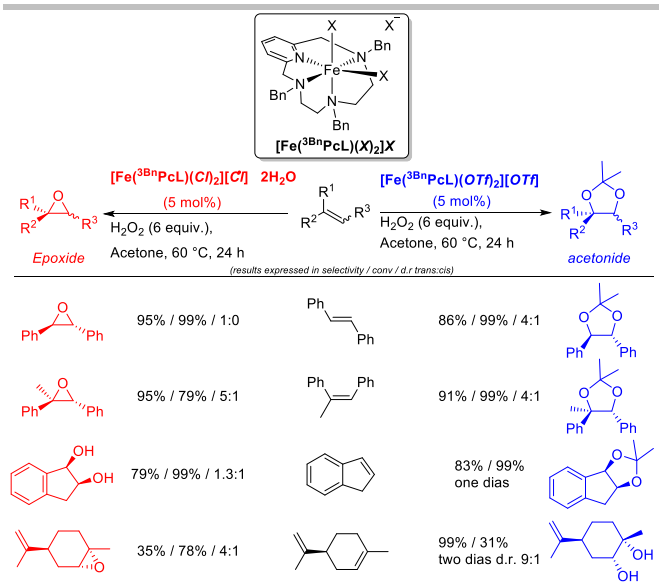

Scheme 30. Limited scope of *syn*-dihydroxylation through Fe^{III} complex.[73]

4.1.4. Asymmetric *syn*-dihydroxylation

Methods for asymmetric catalyzed *cis*-dihydroxylation are rare and this area requires more attention.[7b] With the iron complexes, the situation is even more complicated and we had to wait until 2008 to see the first example described by Que and co-workers.[60c]

A high level of enantioenrichment (up to 97% ee) has been obtained but unfortunately this goes hand in hand with low yields of diols.

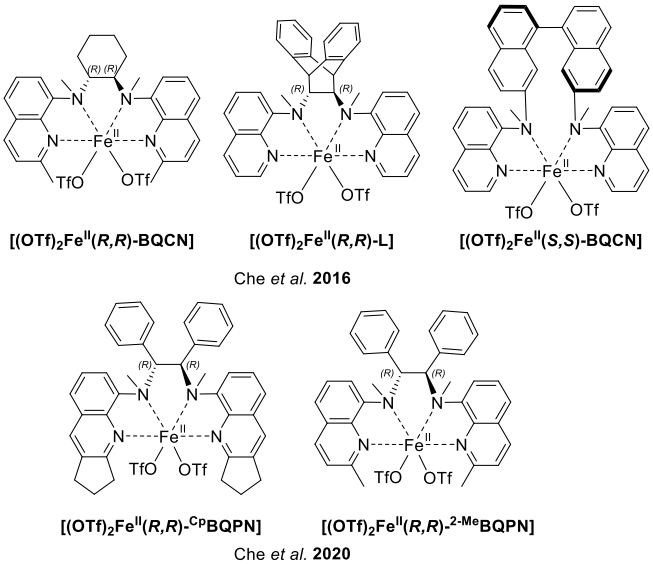

Figure 16. Chiral Fe complexes used in asymmetric *syn*-dihydroxylation.

A significant discovery has been recently disclosed by Che and co-workers.[64] Seven chiral ligands were screened in the asymmetric dihydroxylation with H_2O_2 as oxidant (some of them are depicted in Figure 16). Best results were obtained with complex [Fe(OTf)$_2$(^{6Me2}bqcn)] (3 mol%) for which the formation of *syn*-diols was promoted with high yields and enantioselectivities and the competitive epoxide was formed in less than 1% yield (Scheme 31a). Methanol as solvent was found essential to secure high activity and while keeping very mild conditions. X-ray spectroscopy showed that the [Fe(OTf)$_2$(^{6Me2}bqcn)] complex display a *cis*-α coordination topology and a high spin ferrous center. The (*E*)-olefins produced *syn*-diols with high enantioselectivities (87-98%) along with synthetically useful yields (up to 85%). In contrast, for the (*Z*)-olefins, the enantioselectivities were lower (22−83%ee). It is worth to mention that outstanding results were obtained for electron-deficient aromatic alkenes (up to 89% isolated yield and 99.8% ee). Finally, the unconjugated terminal olefins gave good enantiomeric excess of products (81-92%) while the 1,2-diols derived from styrene are obtained with a low enantioenrichment (15-37% ee). For styrene substrates, the asymmetric induction can be increased by 30% using the ligand of binaphthyl type. The [Fe(OTf)$_2$(^{6Me2}bqcn)] complex prefers to oxidize the electron-poor olefins and therefore has a nucleophilic character which is consistent with the class **B** catalyst. Based on ^{18}O-labeling and ESI-MS data, the authors proposed a mechanism, which seems to involve an iron(III)-hydroperoxo (L_4)Fe^{III}-OOH active species (Scheme 31b).

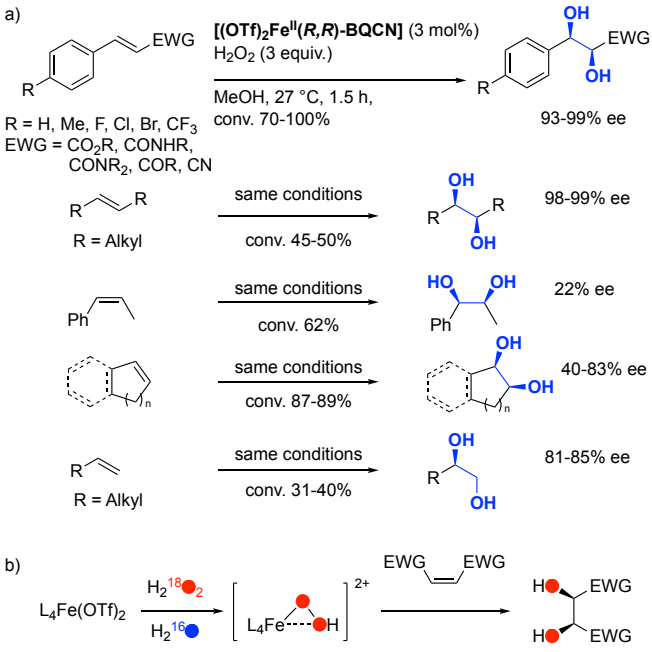

Scheme 31. a) [Fe(OTf)$_2$(^{6Me2}bqcn)]-catalyzed AD of (*E*)- and (*Z*)-alkenes with H_2O_2. b) Key active ferric hydroperoxo species. [64]

Very recently, Che and his colleagues published an iron catalytic system able of oxidizing asymmetrically challenging tri-substituted alkenes substrates.[74] This is a major result because conventionally, the asymmetric dihydroxylation was mainly based on the Sharpless method.[7a, 75] Indeed, these highly congested substrates encounter great difficulties in approaching the coordination sphere of metal catalysts where the oxidation reaction takes place. The author synthesized a new Fe^{II} complex based on tetradentate N_4 bis(quinolyl)diamine type-ligands BQPN (BQPN = (*R,R*)-*N,N'*-dimethyl-*N,N'*-bis(quinolin-8-yl)-1,2-diphenylethane-1,2-diamine) (Figure 16). X-ray crystallographic studies shows that BQPN ligands all adopt a *cis-α* coordination and that the iron center possess a high-spin character.

Using H_2O_2 (3 equiv.) as oxidant and MeOH as solvent in presence of 3 mol% of the α-[Fe^{II}($^{2\text{-Me2}}$-BQPN)$(OTf)_2$], the oxidation of the tri-substituted double bonds proceed with high conversion (70-100%), *cis*-diol selectivity (89-97%) and asymmetric induction (92-99% ee). The electronic and steric effects on the quinolone part of the ligand are detrimental to the activity of the catalyst, but the high enantioselectivities was retained. A large array of alkenes (up to 31 examples), including aliphatic and aromatic (*E*)-alkenes and (Z)-alkenes, were gently converted into the corresponding *cis*-diols by the α-[Fe^{II}($^{2\text{-Me2}}$-BQPN)$(OTf)_2$] catalyst. Excellent enantio- (91.5-99.9% ee) and diols-selectivities (89-99 %) have been obtained for aliphatic (*E*)-alkenes which vary from derivatives of tiglic acid, phenyl senecioate, fumaric acid derivatives, to cyclic alkenes carrying a α-ester group (Scheme 32). For aromatic (*E*)-tri-substituted alkenes such as α- and β-methyl cinnamates, the corresponding diols products were obtained in moderate to high selectivities (65–98%) but still with high enantioselectivity of up to 98.5% ee. Finally, the following (*Z*)-tri-substituted olefins: angélate, angélamide and β-aryle crotonate afforded the *cis*-diols with good-to-excellent enantioselectivities (81-97% ee and 83-90% *cis*-diol selectivities) (Scheme 33).

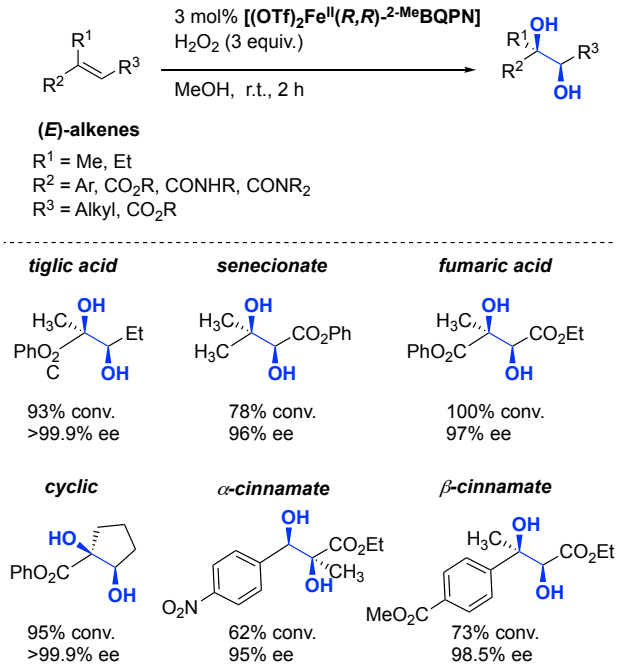

Scheme 32. Aliphatic and aromatic (*E*)-tri-substituted alkenes in the asymmetric *cis*-dihydroxylation catalyzed by [Fe(OTf)$_2$($^{2\text{-Me}}$bqPn)] and H_2O_2. [74]

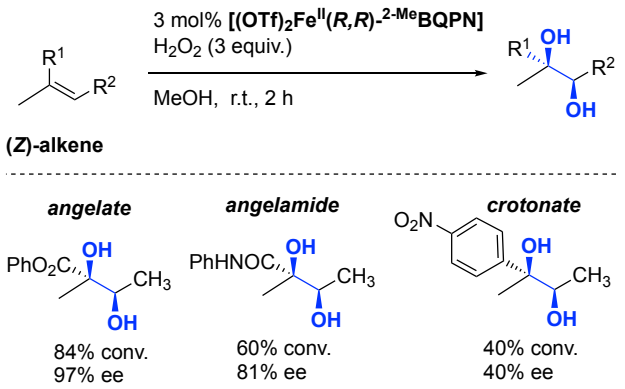

Scheme 33. (*Z*)-tri-substituted alkenes in the asymmetric *cis*-dihydroxylation catalyzed by [Fe(OTf)$_2$($^{2\text{-Me}}$bqPn)] and H_2O_2. [74]

Interestingly gram-scale asymmetric *syn*-dihydroxylation reactions have been successfully performed onto tiglic and fumaric acid derivatives giving respectively 87% and 94% yield along with 99.9% and 97.5% ee. Noteworthy, the Sharpless AD-MIX system generates *cis*-diols with lower yields and reduced enantioselectivities compared to the current Fe(BQPN)/H_2O_2 system. Mechanistic studies using ^{18}O-labeling, UV / Vis, ESI-MS, NMR, EPR and computer studies, advocates to a possible involvement of a *cis*-[Fe^{V}($^{2\text{-Me2}}$-BQPN)$(O)_2$]+ active oxidant which could be generated from the Fe^{III} resting state *via* a non-water assisted pathway. Finally, for fumaric substrates, the author were able to reduce the catalyst loading from 3 mol% to 1 mol% without lost in the asymmetric induction but with slightly lower reactivity.

4.2. O_2 activation

The use of O_2 in catalytic oxidation system arouses great interest because it is an abundant and environmentally benign oxidant. Among several metals iron is known to be able to activate O_2 in heme or nonheme-type ligand environments.[76] However examples of biomimetic iron complexes for oxidation of olefins and aliphatic substrates with dioxygen are rare. This is mainly due to the generation of reactive hydroxyl radical which often leads to the non-selective formation of products and that this non-heme system requires the presence of sacrificial reductants.

Based on the α-keto glutarate-dependent enzymes, the dioxygen reactivity of several well-defined Fe^{II}-α-hydroxy acid complexes attracted some attention. In this case, the active oxidant specie is generated by oxidative decarboxylation of the monoanionic benzilate into benzophenone providing two electrons and one proton to carry the *cis*-dihydroxylation of *cis*-cyclohexene (Figure 17). Paine and co-workers applied this strategy combining α-hydroxy acid with tri- or tetradentate ligands.[61c, 77]. Their first system use an iron(II)-benzilic acid complexes supported by a facial N_3 ligand namely hydrotris(3,5-diphenyl-pyrazol-1-yl)borate ligand (Tp^{Ph2}).[77a] Based on experimental results and DFT calculation the authors proposed that the [(Tp^{Ph2})Fe^{II}(benzilate)] complex generates a nucleophilic iron(III)–hydroperoxo oxidant. Additionally, labelling experiment with $^{18}O_2$ indicates that the oxidant did not exchange its oxygen atoms with water and that the two oxygen atoms on the *cis*-diol

are coming from O_2. Other α-hydroxy acid such mandelic display almost the same activity as the benzylic.[77b] With electron-poor alkenes, the nucleophilic iron-intermediate gives high yield of diols product and lower yields were noticed for electron-rich olefins (Scheme 34). However, styrene substrate affords a mixture of the following oxidized products 1-phenylethane-1,2-diol, benzaldehyde, and benzoic acid in which only 20 % of diol was produced. The authors have shown that the maximum TONs value in diol was reached for a high concentration of alkene (100 equiv. for 10 mL of solvent) in a catalytic system.

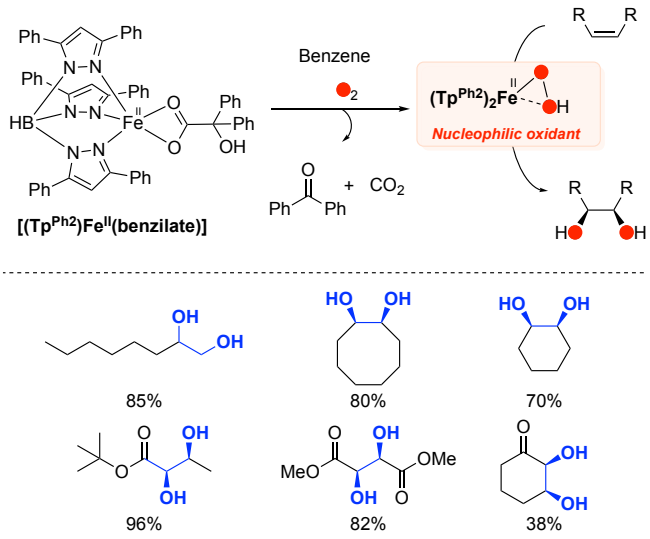

Scheme 34. Nucleophilic oxidant generated from (TP^{Ph2})Fe(benzilate) complexes with O_2 and its reactivity toward alkenes (GC-MS calculated yields).[77a, 77b]

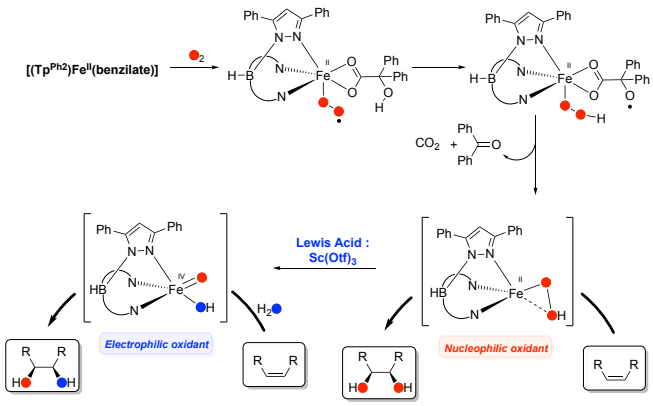

Figure 17. Proposed mechanism for the formation of O_2-derived iron–oxygen oxidants applied to the oxidation of alkenes.

Captivatingly, the addition of Lewis acid such as $Sc(OTf)_3$ in the reaction media switched the character of the oxidant from nucleophile to electrophile.[77c] Labelling experiment using $H_2{}^{18}O$ shows partial incorporation of ^{18}O into the diols (up to 32%). Consequently, under scandium conditions, the diols are obtained with much higher yields from electron-rich alkenes than with electron-deficient alkenes (Scheme 35). The retention of stereochemistry observed for the *cis*-heptene, with or without Sc^{3+}, indicate most probably that the reaction proceeds through a concerted mechanism. Mechanistic studies based on labeling and interception experiments and combined with a DFT calculations indicate a mechanism in which a Lewis acid triggers the heterolytic cleavage of the O−O bond in the iron(II)-hydroperoxide to generate an iron(IV)-oxohydroxo electrophilic oxidant.[77c] This electrophilic oxidant can now exchange its two oxygen atoms, which are in *cis*-arrangement, with a molecule of water.

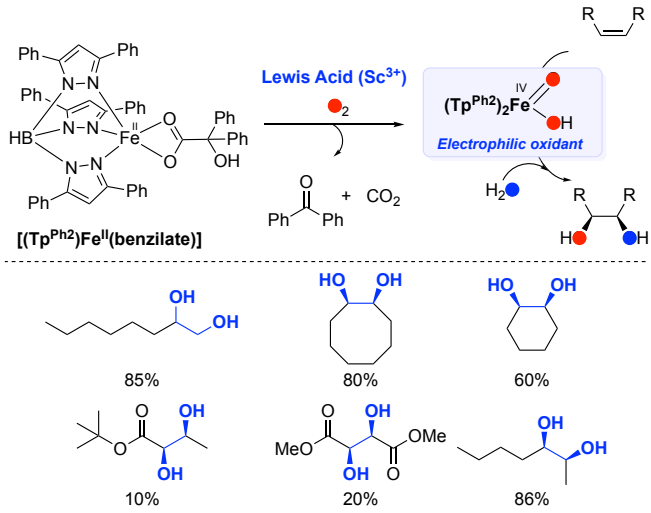

Scheme 35. Electrophilic oxidant generated from (TP^{Ph2})Fe(benzilate) complexes with O_2 and its reactivity toward alkenes. [77c]

Subsequently, Paine and co-workers explored the effect of the topology of several N_4 ligands on the catalytic oxidation of olefins by iron(II) benzilate complexes.[61c] Single-crystal X-ray structural studies of these monocationic iron complexes revealed that, except complex [(benzilate)Fe(TBima)], they all contain a six-coordinate iron center surrounded by one N_4 ligand and one monoanionic benzilate (Figure 18). Interestingly for the complex Fe(tpa) the benzilate ligand is not bidentate, but it coordinates the iron center in a κ^1-fashion mode *via* O^- and a MeOH molecule therefore completes the coordination sphere. The reported average Fe−N distances (2.056−2.415 Å) for these metallic species, are consistent with high-spin iron(II) complexes. Complexes with BPMEN and $^{6\text{-Me}2}$BPMEN ligands adopt a *cis*-α-geometry and NMR analyses sorely suggest that both complexes retain their *cis*-α-topology in solution as well. In contrast, for complex [(benzilate)Fe(TBima)] five atoms bound the central atom in a trigonal-bipyramidal geometry including a monodentate benzilate.

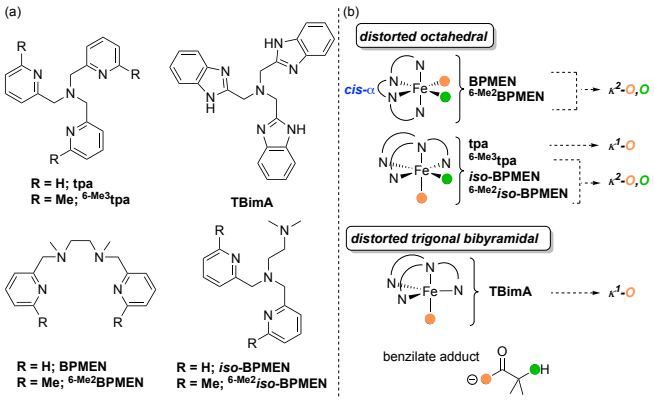

Figure 18. (a) Tetradentate N_4 ligand discussed in this review. (b) Coordination geometry of (N_4)Fe(II)benzilate complexes. [61c]

Using 100 equiv. of alkenes in presence of molecular O_2 only complexes Fe($^{6\text{-Me}3}$tpa), Fe(BPMEN), Fe($^{6\text{-Me}2}$BPMEN), Fe(*iso*-BPMEN) and Fe(*iso*-$^{6\text{-Me}2}$BPMEN) are capable of forming *cis*-diols but only with moderate yields (Scheme 36). For styrene, the formation of the diol has always been accompanied by the product of overoxidation (benzoic acid).[61c] It is noteworthy that compared to Fe(Tp^{Ph2}), the tetradentate iron complexes react slowly with O_2 and the reactions need a few hours to quantitative decarboxylation of benzilate. A labeling experiment with 1-octene substrate with Fe($^{6\text{-Me}3}$tpa) reveals that both of the oxygen atoms come from molecular O_2 and that they do not exchange with water. This unambiguously suggests the formation of nucleophilic iron(II) hydroperoxides oxidant. DFT calculation shows that upon the nature of the ligand different geometries were preferred for the iron(II)hydroperoxides. The $^{6\text{-Me}3}$tpa, $^{6\text{-Me}2}$*iso*-BPMEN, BPMEN, and $^{6\text{-Me}2}$BPMEN promote the formation of more stable high spin side-on $[(L)Fe^{II}(OOH)]^+$ complexes in which the two oxygen atoms bound the iron center, while for the ligands TPA, iso-BPMEN and TBimA, the high spin end-on geometry is favoured, in this case, only one oxygen atom is attached to the metal. Interestingly, only side-on iron(II)hydroperoxides afford a *cis*-diol product in reactions with olefins.

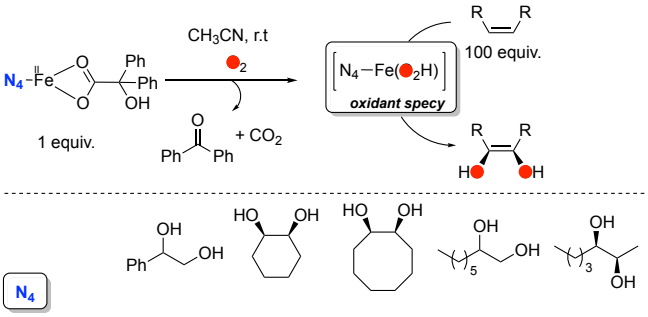

$^{6\text{-Me}3}$tpa	17%	20%	16%	12%	29%
$^{6\text{-Me}2}$*iso*-BPMEN	35%	-	-	-	-
BPMEN	16%	12%	<5%	<5%	-
$^{6\text{-Me}2}$BPMEN	42%	<10%	12%	21%	24%
TPA, iso-BPMEN, TBimA	no product				

Scheme 36. Evaluation of Iron(II) Benzilate complexes in *syn*-dihydroxylation with dioxygen[61c]

More recently, the same authors showed that the replacement of the phenyl group by a methyl on the three pyrazole cores of the ligand is beneficial and it leads to a slight increase in yields of 5 to 10% in diols.[77d] Under stoichiometric conditions, this $TP^{Ph,Me}$ ligand did not show detectable intraligand hydroxylation which led to the development of a catalytic system which used only an excess of benzilate. Under catalytic conditions, diols were generated with good to high yields (80-96%) (Scheme 37). Under the experimental conditions, the highest catalytic activity was observed with Fe($Tp^{Me,Ph}$), affording 17 turnovers for the conversion for octane-1,2-diol; which contrasts with the low 1.3 TON reported for the Fe(Tp^{Ph2})complexes. The use of additives shows that the addition of pyridine or tetrabutylammonium hydroxide has completely inhibited the formation of diol and the alkenes are oxidized to corresponding epoxides albeit with lower catalytic activity. However, addition of Sc^{3+} did not influence the yield but it increases the TONs of octane-1,2-diol up to 21. Based on labeling and interception experiments , the authors propose for the oxidation reactions that an iron−oxygen oxidants species (i) iron(II)-hydroperoxide is involved when there is no external additive, (ii) iron(IV)-oxo-hydroxo is involved when there is a Lewis acid, (iii) with protic acid, a new iron(IV)-oxo-aqua species is proposed as being the active oxidant but it favors in olefin epoxidation reaction instead of *cis*-dihydroxylation.[77d]

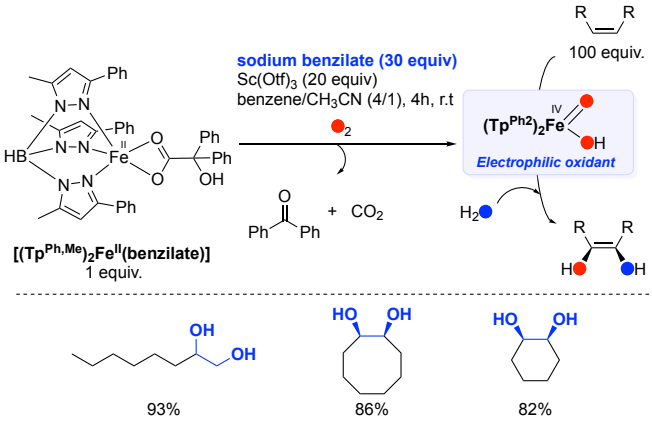

Scheme 37. Electrophilic oxidant generated from (TP^{Ph2})Fe(benzilate) complexes with O_2. [77d]

Finally, an iron (II) benzilate complex modified with TPA ligand was immobilized on gold nanoparticles stabilized with octanethiol, but this approach hindered the *cis*-dihydroxylation of alkenes and only 1-octene as substrate produced the diol (with 35% yield).[77e]

5. Other transition metal complexes capable of promoting the *syn*-dihydroxylation of alkenes

Other direct *syn*-dihydroxylation procedures involving other transition metals than those already mentioned in this review are described but there are far fewer methods previously described. They mainly involved Mo,[78] Pd[79] or Tc[80] as catalysts and since 2010, the palladium methods only have been slightly extended.

5.1. Palladium-mediated *syn*-dihydroxylation & diacetoxylation

Straight synthesis of *syn*-diol using palladium catalyst is scarce and most often, due to the experimental conditions, the acetoxyhydroxylation or diacetoxylation reactions preferably take place.[79c, 81]

5.1.1. Indirect *syn*-dihydroxylation *via syn*-acetoxyhydroxylation

Shi *et al.* have successfully applied a Pd^{II}/Pd^{IV} catalytic system, using bis-(NHC)–Pd(II) complexes to dioxygenate alkenes, leading to the formation of a mixture of *syn*-hydroxyacetate (Major) and diacetylated compounds (Scheme 38).[79b] $PhI(OAc)_2$ is used as an oxidant and the presence wet acetic acid is necessary to achieve high conversions. Final acetylation was complete by addition of an excess of acetic anhydride to generate the protected diols in good yields and good diastereoselectivities. The authors suggested a "S_N2 type" elimination with inversion of the configuration resulting either from an intramolecular or intermolecular attack of an acetate ligand to justify the *syn*-selectivity observed.

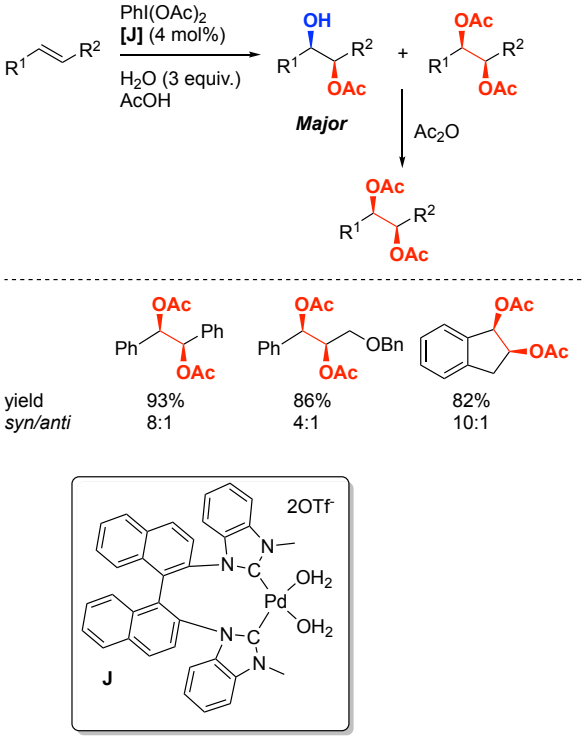

Scheme 38. *Syn*- acetoxyhydroxylation of olefins catalyzed by NHC-Pd catalyst **J**.[79b]

Kang and co-workers recently described a direct acetoxyhydroxylation of terminal olefin catalyzed by $Pd(CH_3CN)_2(NO_2)_2$ (7 mol%) and *tert*-butyl nitrite (*t*BuONO, 20 mol%) system under air/O_2.[82] Depending on the reaction conditions, the acetoxyhydroxylation intermediates generate the corresponding vicinal diols under hydrolysis conditions with K_2CO_3 or provide the diacetoxy-products under acetylating conditions (Scheme 38). Vicinal diols were obtained in good yield and the system is tolerant to a wide range of functional group (amide, benzyloxy, bromo, TBDPS, carbonyl, and sulfonyl). However, this procedure is limited to terminal alkenes and both internal and deactivated olefins did not generate the acetoxyhydroxylation product. The reaction has been successfully extended to the gram scale for 10-undecenoic acid substrate giving 83% (1.4 g) of diol.

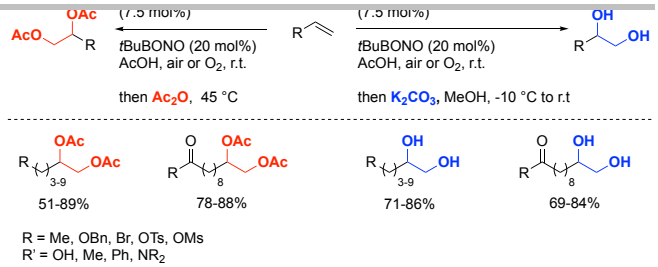

Scheme 39. Diacetoxylation or dihydroxylation of terminal alkenes catalysed by Pd complex under *t*BuONO/O_2.[82]

5.1.2. Direct *syn*-dihydroxylation

Inspired by their work on the diacetoxylation reaction, Jiang and co-workers have proposed the only direct preparation to date of 1,2-diols, under aerobic conditions (Scheme 40).[79a] The reaction simply used palladium(II) acetate (4 mol%) as catalyst in water under basic conditions with oxygen (8 atm) as oxidant. The presence of base was crucial to circumvent the oxidative cleavage of olefin observed in acidic media. A wide range of olefins (terminal and *cis*- or *trans*-1,2-disubstituted alkenes) have been selectively oxidized to the corresponding *cis*-1,2-diols in good yields, but the 8 Atm of O_2 pressure used still represents a main drawback. Finally, large scale-synthesis was easily set up using up to 100 mmol of styrene.

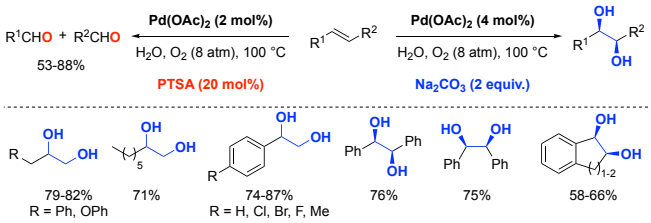

Scheme 40. Palladium catalysed alkene *syn*-dihydroxylation and alkene cleavage reaction.[79a]

6. Conclusion

In this mini-review, advances in the field of *syn*-dihydroxylation of olefins were highlighted and organized according to the type of metal. Even if osmium-mediated *syn*-dihydroxylation still represents a large part of the reported procedures, the last decade has seen the emergence of osmium-free alternatives using environmentally benign oxidants. In particular, most of the recent extension was carried out with iron complexes.

However, several problems need to be resolved in order to extend the use of these catalysts in practical *syn*-dihydroxylation: (i) the quest for more active catalysts providing improved yields and selectivities are necessary for the electron-rich olefins which prefer to generate the undesired epoxide, (ii) access to a simpler and more modular ligand framework or to more convenient synthetic route will be desirable for synthetic applications, (iii) as a general issue the substrate scope and functional group tolerance still need to be expanded to further

application in syntheses of more sophisticated architectures and (iv) the strong oxidizing power of alternative metal centers must be controlled and modulated to be compatible with the milder experimental requirement of asymmetric version. The last results reported for manganese and very recently by Che and co-workers for non-heme iron should encourage scientist to explore and propose new asymmetric version on this *syn*-dihydroxylation to bring this catalytic chiral transformation much closer to practical applications.
In view of the results of the last 10 years we can only be enthusiastic about the future and the development of such oxidative reaction.

Acknowledgements

The authors thank the CNRS and the University of Strasbourg for financial support.

Keywords: *syn*-dihydroxylation •1,2-diols • *syn*-oxidation • metal-catalysis • asymmetric catalysis

[1] (a) A. Helenius, M. Aebi, *Science* **2001**, *291*, 2364-2369; (b) Y. van Kooyk, G. A. Rabinovich, *Nat. Immunol.* **2008**, *9*, 593-601; (c) M. L. A. de Leoz, H. J. An, S. Kronewitter, J. Kim, S. Beecroft, R. Vinall, S. Miyamoto, R. D. White, K. S. Lam, C. Lebrilla, *Disease Markers* **2008**, *25*, 243-258.

[2] (a) A. C. WeymouthWilson, *Nat. Prod. Rep.* **1997**, *14*, 99-110; (b) A. P. McCaffrey, L. Meuse, T. T. T. Pham, D. S. Conklin, G. J. Hannon, M. A. Kay, *Nature* **2002**, *418*, 38-39.

[3] M. S. Butler, *Nat. Prod. Rep.* **2008**, *25*, 475-516.

[4] H. B. Kagan, in *Asymmetric Synthesis* (Ed.: J. D. Morrison), Academic Press, San Diego, **1985**, pp. 1-39.

[5] K. A. Hofmann, Ber. Dtsch. Chem. Ges. 1912, 45, 3329.

[6] R. Criegee, B. Marchand, H. Wannowius, *Liebigs Ann. Chem.* **1942**, *550*, 99-133.

[7] (a) H. C. Kolb, M. S. Vannieuwenhze, K. B. Sharpless, *Chem. Rev.* **1994**, *94*, 2483-2547; (b) R. V. Ottenbacher, E. P. Talsi, K. P. Bryliakov, *Russ. Chem. Rev.* **2019**, *88*, 1094-1103.

[8] C. J. R. Bataille, T. J. Donohoe, *Chem. Soc. Rev.* **2011**, *40*, 114-128.

[9] M. J. Rawling, N. C. O. Tomkinson, *Org. Biomol. Chem.* **2013**, *11*, 1434-1440.

[10] (a) V. V. Zhdankin, R. Tykwinski, B. Berglund, M. Mullikin, R. Caple, N. S. Zefirov, A. S. Kozmin, *J. Org. Chem.* **1989**, *54*, 2609-2612; (b) M. Celik, C. Alp, B. Coskun, M. S. Gultekin, M. Balci, *Tetrahedron Lett.* **2006**, *47*, 3659-3663; (c) W. H. Zhong, J. Yang, X. B. Meng, Z. J. Li, *J. Org. Chem.* **2011**, *76*, 9997-10004; (d) W. H. Zhong, S. Liu, J. Yang, X. B. Meng, Z. J. Li, *Org. Lett.* **2012**, *14*, 3336-3339; (e) J. H. Lee, S. Choi, K. B. Hong, *Molecules* **2019**, *24*.

[11] (a) N. V. S. Mudiganti, S. Claessens, P. Habonimana, N. De Kimpe, *J. Org. Chem.* **2008**, *73*, 3867-3874; (b) R. S. Phatake, C. V. Ramana, *Tetrahedron Lett.* **2015**, *56*, 2183-2186.

[12] (a) J. C. Griffith, K. M. Jones, S. Picon, M. J. Rawling, B. M. Kariuki, M. Campbell, N. C. O. Tomkinson, *J. Am. Chem. Soc.* **2010**, *132*, 14409-14411; (b) S. Picon, M. Rawling, M. Campbell, N. C. O. Tomkinson, *Org. Lett.* **2012**, *14*, 6250-6253; (c) M. J. Rawling, J. H. Rowley, M. Campbell, A. R. Kennedy, J. A. Parkinson, N. C. O. Tomkinson, *Chem. Sci.* **2014**, *5*, 1777-1785; (d) R. Zhao, D. Chang, L. Shi, *Synthesis-Stuttgart* **2017**, *49*, 3357-3365; (e) A. Pilevar, A. Hossein, J. Becker, P. R. Schreiner, *J. Org. Chem.* **2019**, *84*, 12377-12386.

[13] (a) T. M. Nguyen, D. Lee, *Org. Lett.* **2001**, *3*, 3161-3163; (b) S. Santoro, C. Santi, M. Sabatini, L. Testaferri, M. Tiecco, *Adv. Synth. Catal.* **2008**, *350*, 2881-2884; (c) L. Yu, J. Wang, T. Chen, K. H. Ding, Y. Pan, *Chinese J. Org. Chem.* **2013**, *33*, 1096-1099; (d) L. X. Shao, Y. M. Li, J. M. Lu, X. F. Jiang, *Org. Chem. Front.* **2019**, *6*, 2999-3041.

[14] Y. Ashikari, T. Nokami, J. Yoshida, *Org. Lett.* **2012**, *14*, 938-941.

[15] A. P. Y. Chan, A. G. Sergeev, *Coord. Chem. Rev.* **2020**, *413,* 213213.

[16] K. B. Sharpless, K. Akashi, *J. Am. Chem. Soc.* **1976**, *98*, 1986-1987.

[17] V. Piccialli, D. M. A. Smaldone, D. Sica, *Tetrahedron* **1993**, *49*, 4211-4228.

[18] (a) T. K. M. Shing, E. K. W. Tam, V. W. F. Tai, I. H. F. Chung, Q. Jiang, *Chem. Eur. J* **1996**, *2*, 50-57; (b) T. K. M. Shing, E. K. W. Tam, *Tetrahedron Lett.* **1999**, *40*, 2179-2180.

[19] (a) B. Plietker, M. Niggemann, *Org. Lett.* **2003**, *5*, 3353-3356; (b) B. Plietker, *Synthesis-Stuttgart* **2005**, 2453-2472; (c) B. Plietker, M. Niggemann, *J. Org. Chem.* **2005**, *70*, 2402-2405.

[20] (a) B. Plietker, M. Niggemann, *Org. Biomol. Chem.* **2004**, *2*, 2403-2407; (b) V. Piccialli, *Molecules* **2014**, *19*, 6534-6582; (c) S. Chittela, T. R. Reddy, P. R. Krishna, S. Kashyap, *J. Org. Chem.* **2015**, *80*, 7108-7116; (d) K. Nandini, P. Srinivas, B. K. Bettadaiah, *Tetrahedron Lett.* **2015**, *56*, 2704-2706; (e) M. Moreaux, G. Bonneau, A. Peru, F. Brunissen, M. Janvier, A. Haudrechy, F. Allais, *Eur. J. Org. Chem.* **2019**, *2019*, 1600-1604.

[21] S. Beligny, S. Eibauer, S. Maechling, S. Blechert, *Angew. Chem. Int. Ed.* **2006**, *45*, 1900-1903.

[22] A. A. Scholte, M. H. An, M. L. Snapper, *Org. Lett.* **2006**, *8*, 4759-4762.

[23] N. M. Neisius, B. Plietker, *J. Org. Chem.* **2008**, *73*, 3218-3227.

[24] M. Malik, G. Witkowski, M. Ceborska, S. Jarosz, *Org. Lett.* **2013**, *15*, 6214-6217.

[25] M. Malik, M. Ceborska, G. Witkowski, S. Jarosz, *Tetrahedron-Asymmetry* **2015**, *26*, 29-34.

[26] M. Malik, S. Jarosz, *Beilstein J. Org. Chem.* **2016**, *12*, 2602-2608.

[27] S. Chittela, T. R. Reddy, P. R. Krishna, S. Kashyap, *RSC Advances* **2014**, *4*, 46327-46331.

[28] R. J. Ferrier, in *Glyoscience: Epimerisation, Isomerisation and Rearrangement Reactions of Carbohydrates, Vol. 215* (Ed.: A. E. Stutz), **2001**, pp. 153-175.

[29] S. Adachi, K. Watanabe, Y. Iwata, S. Kameda, Y. Miyaoka, M. Onozuka, R. Mitsui, Y. Saikawa, M. Nakata, *Angew. Chem. Int. Ed.* **2013**, *52*, 2087-2091.

[30] H. Takamura, K. Tsuda, Y. Kawakubo, I. Kadota, D. Uemura, *Tetrahedron Lett.* **2012**, *53*, 4317-4319.

[31] H. Kawamoto, Y. Ohmori, M. Maekawa, M. Shimada, N. Mano, T. Iida, *Chem. Phys. Lipids* **2013**, *175*, 73-78.

[32] W. P. Yip, W. Y. Yu, N. Y. Zhu, C. M. Che, *J. Am. Chem. Soc.* **2005**, *127*, 14239-14249.

[33] W. P. Yip, C. M. Ho, N. Zhu, T. C. Lau, C. M. Che, *Chem-Asian J.* **2008**, *3*, 70-77.

[34] C. W. Tse, Y. G. Liu, T. W. S. Chow, C. Q. Ma, W. P. Yip, X. Y. Chang, K. H. Low, J. S. Huang, C. M. Che, *Chem. Sci.* **2018**, *9*, 2803-2816.

[35] (a) T. P. Montgomery, A. M. Johns, R. H. Grubbs, *Catalysts* **2017**, *7*; (b) A. W. M. Lee, W. H. Chan, W. H. Yuen, P. F. Xia, W. Y. Wong, *Tetrahedron-Asymmetry* **1999**, *10*, 1421-1424.

[36] (a) A. Kekulé and R. Anschütz, Ber. Dtsch. Chem. Ges., 1881, 14, 713–717; (b) A. Kekulé and R. Anschütz, Ber. Dtsch. Chem. Ges., 1880, 13, 2150–2152; (c) S. Tanatar, Ber. Dtsch. Chem. Ges., 1879, 12, 2293–2298.

[37] Modern Oxidation Methods, 2nd ed. J.-E. Bäckvall, Wiley-VCH Verlag GmbH & Co. KGaA, 2011

[38] S. Dash, S. Patel, B. K. Mishra, *Tetrahedron* **2009**, *65*, 707-739.

[39] D. Dalmizrak, H. Goksu, M. S. Gultekin, *RSC Advances* **2015**, *5*, 20751-20755.

[40] J. K. Cha, N. S. Kim, *Chem. Rev.* **1995**, *95*, 1761-1795.

[41] Z. B. Luo, C. Zhao, J. M. Xie, H. F. Lu, *Synthesis-Stuttgart* **2016**, *48*, 3696-3700.

[42] I. Khan, Z. B. Luo, A. Valeru, Y. Xu, B. Liu, B. Sangepu, J. M. Xie, *Synthesis-Stuttgart* **2018**, *50*, 1815-1819.

[43] R. A. Bhunnoo, Y. L. Hu, D. I. Laine, R. C. D. Brown, *Angew. Chem. Int. Ed.* **2002**, *41*, 3479-3480.

[44] (a) C. Wang, L. L. Zong, C. H. Tan, *J. Am. Chem. Soc.* **2015**, *137*, 10677-10682; (b) L. L. Zong, C. H. Tan, *Acc. Chem. Res.* **2017**, *50*, 842-856.

[45] D. E. De Vos, S. de Wildeman, B. F. Sels, P. J. Grobet, P. A. Jacobs, *Angew. Chem. Int. Ed.* **1999**, *38*, 980-983.

[46] (a) J. Brinksma, L. Schmieder, G. van Vliet, R. Boaron, R. Hage, D. E. De Vos, P. L. Alsters, B. L. Feringa, *Tetrahedron Lett.* **2002**, *43*, 2619-2622; (b) J. W. de Boer, J. Brinksma, W. R. Browne, A. Meetsma, P. L. Alsters, R. Hage, B. L. Feringa, *J. Am. Chem. Soc.* **2005**, *127*, 7990-7991; (c) J. W. de Boer, W. R. Browne, J. Brinksma, P. L. Alsters, R. Hage, B. L. Feringa, *Inorg. Chem.* **2007**, *46*, 6353-6372; (d) J. W. de Boer, P. L. Alsters, A. Meetsma, R. Hage, W. R. Browne, B. L. Feringa, *Dalton Trans.* **2008**, 6283-6295; (e) J. W. de Boer, W. R. Browne, S. R. Harutyunyan, L. Bini, T. D. Tiemersma-Wegman, P. L. Alsters, R. Hage, B. L. Feringa, *Chem. Commun.* **2008**, 3747-3749; (f) P. Saisaha, D. Pijper, R. P. van Summeren, R. Hoen, C. Smit, J. W. de Boer, R. Hage, P. L. Alsters, B. L. Feringa, W. R. Browne, *Org. Biomol. Chem.* **2010**, *8*, 4444-4450.

[47] (a) N. J. Schoenfeldt, A. W. Korinda, J. M. Notestein, *Chem. Commun.* **2010**, *46*, 1640-1642; (b) N. J. Schoenfeldt, Z. J. Ni, A. W. Korinda, R. J. Meyer, J. M. Notestein, *J. Am. Chem. Soc.* **2011**, *133*, 18684-18695; (c) N. J. Schoenfeldt, J. M. Notestein, *Acs Catalysis* **2011**, *1*, 1691-1701; (d) K. R. Bjorkman, N. J. Schoenfeldt, J. M. Notestein, L. J. Broadbelt, *J. Catal.* **2012**, *291*, 17-25.

[48] A. Nodzewska, A. Wadolowska, M. Watkinson, *Coord. Chem. Rev.* **2019**, *382*, 181-216.

[49] D. Pijper, P. Saisaha, J. W. de Boer, R. Hoen, C. Smit, A. Meetsma, R. Hage, R. P. van Summeren, P. L. Alsters, B. Feringa, W. R. Browne, *Dalton Trans.* **2010**, *39*, 10375-10381.

[50] J. J. Dong, P. Saisaha, T. G. Meinds, P. L. Alsters, E. G. Ijpeij, R. P. van Summeren, B. Mao, M. Fananas-Mastral, J. W. de Boer, R. Hage, B. L. Feringa, W. R. Browne, *Acs Catalysis* **2012**, *2*, 1087-1096.

[51] P. Saisaha, J. J. Dong, T. G. Meinds, J. W. de Boer, R. Hage, F. Mecozzi, J. B. Kasper, W. R. Browne, *Acs Catalysis* **2016**, *6*, 3486-3495.

[52] P. Saisaha, J. W. de Boer, W. R. Browne, *Chem. Soc. Rev.* **2013**, *42*, 2059-2074.

[53] K. P. Bryliakov, *Chem. Rev.* **2017**, *117*, 11406-11459.

[54] T. W. S. Chow, Y. G. Liu, C. M. Che, *Chem. Commun.* **2011**, *47*, 11204-11206.

[55] (a) E. G. Kovaleva, J. D. Lipscomb, *Nat. Chem. Biol.* **2008**, *4*, 186-193; (b) A. J. Jasniewski, L. Que, *Chem. Rev.* **2018**, *118*, 2554-2592.

[56] (a) D. R. Nelson, *J. Am. Chem. Soc.* **2005**, *127*, 12147-12148; (b) D. Mansuy, *C. R. Chim.* **2007**, *10*, 392-413; (c) M. M. Pereira, L. D. Dias, M. J. F. Calvete, *Acs Catalysis* **2018**, *8*, 10784-10808.

[57] L. Vicens, G. Olivo, M. Costas, *ACS Catalysis* **2020**, *10*, 8611-8631.

[58] (a) G. Olivo, O. Cusso, M. Costas, *Chem-Asian J.* **2016**, *11*, 3148-3158; (b) G. Olivo, O. Cusso, M. Borrell, M. Costas, *J. Biol. Inorg. Chem.* **2017**, *22*, 425-452; (c) S. Kal, S. Xu, L. Que Jr., *Angew. Chem. Int. Ed.* **2020**, *59*, 7332-7349.

[59] (a) K. Chen, L. Que, *Angew. Chem. Int. Ed.* **1999**, *38*, 2227-2229; (b) K. Chen, M. Costas, J. H. Kim, A. K. Tipton, L. Que, *J. Am. Chem. Soc.* **2002**, *124*, 3026-3035; (c) J. Y. Ryu, J. Kim, M. Costas, K. Chen, W. Nam, L. Que, *Chem. Commun.* **2002**, 1288-1289.

[60] (a) P. D. Oldenburg, A. A. Shteinman, L. Que, *J. Am. Chem. Soc.* **2005**, *127*, 15672-15673; (b) P. D. Oldenburg, C. Y. Ke, A. A. Tipton, A. A. Shteinman, L. Que, *Angew. Chem. Int. Ed.* **2006**, *45*, 7975-7978; (c) K. Suzuki, P. D. Oldenburg, L. Que, *Angew. Chem. Int. Ed.* **2008**, *47*, 1887-1889; (d) P. D. Oldenburg, Y. Feng, I. Pryjomska-Ray, D. Ness, L. Que, *J. Am. Chem. Soc.* **2010**, *132*, 17713-17723.

[61] (a) M. Costas, L. Que, *Angew. Chem. Int. Ed.* **2002**, *41*, 2179-2181; (b) R. Mas-Balleste, M. Costas, T. van den Berg, L. Que, *Chem. Eur. J* **2006**, *12*, 7489-7500; (c) B. Chakraborty, R. D. Jana, R. Singh, S. Paria, T. K. Paine, *Inorg. Chem.* **2017**, *56*, 359-371.

[62] (a) K. P. Bryliakov, E. P. Talsi, *Coord. Chem. Rev.* **2014**, *276*, 73-96; (b) W. N. Oloo, L. Que, *Acc. Chem. Res.* **2015**, *48*, 2612-2621.

[63] (a) A. Bassan, M. R. A. Blomberg, P. E. M. Siegbahn, L. Que, *Angew. Chem. Int. Ed.* **2005**, *44*, 2939-2941; (b) I. Prat, J. S. Mathieson, M. Guell, X. Ribas, J. M. Luis, L. Cronin, M. Costas,

Nat. Chem. **2011**, *3*, 788-793; (c) M. Borrell, E. Andris, R. Navratil, J. Roithova, M. Costas, *Nat. Commun.* **2019**, *10*.

[64] C. Zang, Y. G. Liu, Z. J. Xu, C. W. Tse, X. G. Guan, J. H. Wei, J. S. Huang, C. M. Che, *Angew. Chem. Int. Ed.* **2016**, *55*, 10253-10257.

[65] I. Prat, A. Company, T. Corona, T. Parella, X. Ribas, M. Costas, *Inorg. Chem.* **2013**, *52*, 9229-9244.

[66] I. Prat, D. Font, A. Company, K. Junge, X. Ribas, M. Beller, M. Costas, *Adv. Synth. Catal.* **2013**, *355*, 947-956.

[67] P. Spannring, I. Prat, M. Costas, M. Lutz, P. C. A. Bruijnincx, B. M. Weckhuysen, R. Gebbink, *Catal. Sci.Technol.* **2014**, *4*, 708-716.

[68] S. R. Iyer, M. M. Javadi, Y. Feng, M. Y. Hyun, W. N. Oloo, C. Kim, L. Que, *Chem. Commun.* **2014**, *50*, 13777-13780.

[69] A. Kejriwal, S. Biswas, A. N. Biswas, P. Bandyopadhyay, *J. Mol. Catal. A: Chem.* **2016**, *413*, 77-84.

[70] T. W. S. Chow, E. L. M. Wong, Z. Guo, Y. G. Liu, J. S. Huang, C. M. Che, *J. Am. Chem. Soc.* **2010**, *132*, 13229-13239.

[71] M. Borrell, M. Costas, *J. Am. Chem. Soc.* **2017**, *139*, 12821-12829.

[72] M. Borrell, M. Costas, *ACS Sustainable Chem. Eng.* **2018**, *6*, 8410-8416.

[73] G. Tseberlidis, L. Demonti, V. Pirovano, M. Scavini, S. Cappelli, S. Rizzato, R. Vicente, A. Caselli, *ChemCatChem* **2019**, *11*, 4907-4915.

[74] J. Wei, L. Wu, H.-X. Wang, X. Zhang, C.-W. Tse, C.-Y. Zhou, J.-S. Huang, C.-M. Che, *Angew. Chem. Int. Ed.*, *n/a*.

[75] K. Morikawa, J. Park, P. G. Andersson, T. Hashiyama, K. B. Sharpless, *J. Am. Chem. Soc.* **1993**, *115*, 8463-8464.

[76] S. Sahu, D. P. Goldberg, *J. Am. Chem. Soc.* **2016**, *138*, 11410-11428.

[77] (a) S. Paria, L. Que, T. K. Paine, *Angew. Chem. Int. Ed.* **2011**, *50*, 11129-11132; (b) S. Paria, S. Chatterjee, T. K. Paine, *Inorg. Chem.* **2014**, *53*, 2810-2821; (c) S. Chatterjee, T. K. Paine, *Angew. Chem. Int. Ed.* **2015**, *54*, 9338-9342; (d) S. Chatterjee, S. Bhattacharya, T. K. Paine, *Inorg. Chem.* **2018**, *57*, 10160-10169; (e) D. Sheet, A. Bera, R. D. Jana, T. K. Paine, *Inorg. Chem.* **2019**, *58*, 4828-4841.

[78] (a) A. V. Biradar, B. R. Sathe, S. B. Umbarkar, M. K. Dongare, *J. Mol. Catal. A-Chem* **2008**, *285*, 111-119; (b) P. Chandra, S. L. Pandhare, S. B. Umbarkar, M. K. Dongare, K. Vanka, *Chem. Eur. J* **2013**, *19*, 2030-2040.

[79] (a) A. Wang, H. F. Jiang, *J. Org. Chem.* **2010**, *75*, 2321-2326; (b) W. F. Wang, F. J. Wang, M. Shi, *Organometallics* **2010**, *29*, 928-933; (c) S. E. Mann, L. Benhamou, T. D. Sheppard, *Synthesis-Stuttgart* **2015**, *47*, 3079-3117.

[80] R. M. Pearlstein, A. Davison, *Polyhedron* **1988**, *7*, 1981-1989.

[81] (a) S. Enthaler, A. Company, *Chem. Soc. Rev.* **2011**, *40*, 4912-4924; (b) M. Hu, W. Q. Wu, H. F. Jiang, *Chemsuschem* **2019**, *12*, 2911-2935.

[82] X. M. Chen, X. S. Ning, Y. B. Kang, *Org. Lett.* **2016**, *18*, 5368-5371.